

# Molecular response to multiple trace element contamination of the European sardine

Anaïs Beauvieux<sup>1</sup>, Jean-Marc Fromentin<sup>1</sup>, Claire Saraux<sup>2</sup>, Diego Romero<sup>3</sup>, Nathan Couffin<sup>2,4</sup>, Adrien Brown<sup>2,4</sup>, Luisa Metral<sup>1</sup>, Fabrice Bertile<sup>2,4</sup>, Quentin Schull<sup>1</sup>

<sup>1</sup> MARBEC, Univ Montpellier, CNRS, Ifremer, IRD, Sète, France

<sup>2</sup> Université de Strasbourg, CNRS, IPHC UMR 7178, F-67000 Strasbourg, France

<sup>3</sup> Toxicology Department, Faculty of Veterinary Medicine, University of Murcia, 30100 Murcia, Spain

<sup>4</sup> Infrastructure Nationale de Protéomique ProFI, FR2048 CNRS CEA, Strasbourg 67087, France

\*Corresponding author

Correspondence: [anaïs.beauvieux@gmail.com](mailto:anaïs.beauvieux@gmail.com)

## ABSTRACT

In marine ecosystems, the presence of trace elements resulting from anthropogenic activities has raised concerns regarding their potential effects on marine organisms. This study delves into the intricate relationship between trace element contamination and the physiological responses of a key marine species in the Mediterranean Sea: the European sardine. Since 2008, this species has been experiencing a significant crisis in the region, prompting numerous studies to investigate the potential factors behind the dramatic decline in sardines' size, age, and body condition. However, thorough information on chemical contamination by trace elements and its physiological impact on this species was lacking. We found evidence for the accumulation of multiple elements in sardines, with a light East-West contamination gradient within the Gulf of Lions. While macro-physiological parameters (i.e. body condition) were not affected by contamination, pathways involved in cellular organization and response to stress were clearly upregulated, particularly in the liver, but also in muscle. In addition, a global upregulation in processes linked to the immune system, lipid homeostasis and oxidative stress was recorded in the liver. The associated energetic cost may add a substantial burden to sardines that already face multi-factorial constraints. This study also allows to pinpoint biomarkers of exposure and effects that may be important for monitoring Mediterranean sardine's health. The results of this study and particularly the complex changes in protein expression demonstrate the need for future studies to test the concomitant effects of multiple stressors acting simultaneously, including large scale contamination.

**Keywords:** Cocktail effect, Ecotoxicology, Gulf of Lions, *Sardina pilchardus*, Shotgun proteomic

44 The Mediterranean Sea suffers from high levels of pollution, making it one of the most polluted seas  
45 in the world (Gabrielides 1995; Danovaro 2003; Sharma et al., 2021; Robledo Ardila et al., 2024). The  
46 sea's semi-enclosed nature contributes to the accumulation of pollutants, exacerbated by significant  
47 atmospheric inputs such as Saharan dust events, intense human activities (Bucchia et al., 2015; Pedrotti  
48 et al., 2016) and riverine outflows on the continental shelves (Durrieu de Madron et al., 2011). This is also  
49 intimately linked to the enhanced ability of pelagic food chains to bioaccumulate chemical elements in  
50 oligotrophic seas such as the Mediterranean Sea (Harmelin-Vivien et al., 2009; Chauvelon et al., 2018).  
51 Among natural and anthropogenic pollutants, trace elements are present in all environmental  
52 compartments. Some metals (e.g., Copper, Feiron, Zinc) are essential for maintaining the healthy  
53 function of the cells of all living organisms, particularly due to their role as components or co-factors of  
54 different enzymes (Wood et al., 2011). Nonetheless, such elements can become toxic when they exceed  
55 certain concentration thresholds, leading to important detrimental effects on the health of organisms  
56 (Plum et al., 2010; Dydak et al., 2011; Asaduzzaman et al., 2017). In addition, non-essential trace/heavy  
57 metals, such as leadPb, mercuryHg, cadmiumCd, arsenicAs, nickelNi, can cause several types of  
58 pathological damage at very low concentration (Friberg et al., 1979; Tchounwou et al., 2012; Jaishankar  
59 et al., 2014). The accumulation of these chemicals can influence enzymatic and metabolic activities,  
60 disrupting ion homeostasis, reducing growth and adversely affecting body condition and swimming  
61 performances (Hollis et al., 1999; Bervoets and Blust 2003; Bervoets et al., 2005). Metals are in fact  
62 inducers of oxidative stress in many animals (including fish), causing imbalances between the production  
63 of reactive oxygen species (ROS) (e.g.  $H_2O_2$ ,  $HO^\bullet$ ,  $O_2^{\cdot-}$ , R, ROO) and cell antioxidant activity (Halliwell &  
64 Gutteridge, 2015). Increased ROS due to overproduction and/or the inability to destroy them may  
65 damage DNA structures and therefore alter the expression patterns of important proteins, hormones,  
66 enzymes, etc. (Morcillo et al., 2016; Javed et al., 2017). Metal contamination also modifies the expression  
67 of proteins (biomarkers) linked to cellular responses to stress and cell detoxification. The use of  
68 biomarkers, such as antioxidant enzymes (Pereira et al., 2013; Williams and Yoshida-Honmachi 2013),  
69 heat shock proteins (HSPs, Downs et al., 2006) and metallothioneins (Sakuragui et al., 2013; Williams and  
70 Yoshida-Honmachi 2013) to monitor metal pollution has been widely accepted in environmental and  
71 ecotoxicology programs.

72 While experimental data under controlled conditions taught us a lot on the molecular and  
73 physiological costs of single contaminants (Isani et al., 2009; Souid et al., 2015; Wang et al., 2013), the  
74 challenge that ecologists now face is to understand the effects of trace element mixtures. Indeed, wildlife  
75 species are continuously and increasingly exposed to a large number of different chemicals at the same  
76 time (Heys et al., 2016). Therefore, the ecotoxicological impacts of trace element mixtures are relatively  
77 less understood. Even at low concentrations, trace elements mixed in the environment can have a  
78 combined toxicological effect (Heys et al., 2016) forming "reactive chemical cocktails" that explain the  
79 synergistic effects of the combination of distinct elements (Kaushal et al., 2018). Considering the effects  
80 of only one pollutant at a time can therefore lead to misinterpretation of biomarker data (Celander,  
81 2011).

82 The emergence of omics tools has provided a potent means of analyzing complex and integrated  
83 responses to contaminants. These tools offer high sensitivity and excellent specificity in studying the  
84 molecular changes occurring in organisms (Denslow et al., 2005; Benninghoff 2007). Additionally, high-  
85 throughout shotgun proteomics (i.e. the direct and rapid analysis of the entire protein compartment  
86 within a complex mixture) provides a unique opportunity to comprehensively examine the expression of  
87 thousands of proteins in a specific tissue in a single experiment, using mass spectrometry and  
88 bioinformatics techniques instead of traditional biochemical methods (Sanchez et al., 2011; López-  
89 Pedrouso et al., 2020). This advance considerably improves our understanding at the protein level and  
90 further paves the way for identifying new biomarkers of exposure and effect, which can then be used to  
91 develop enhanced monitoring programs to better assess the impacts of pollutants on marine species  
92 (Apraiz et al., 2006; Benninghoff 2007).

93 We applied a quantitative proteomics approach to the European sardine (*Sardina pilchardus*) in the  
94 northwestern Mediterranean Sea. This small pelagic fish population has indeed shown a drastic decrease  
95 in size and body condition since 2008 (Van Beveren et al., 2014), resulting in a lower value on the stalls,

96 which in turn has led to the collapse of the French small pelagic fish fisheries, which landed less than 200  
97 tons in 2022 against 15,000 tons in the early 2000s (Van Beveren et al., 2016). The hypotheses of top-  
98 down control through overfishing or natural predation or epizootic diseases have been refuted (Van  
99 Beveren et al., 2016b, 2017, Queiros et al., 2018). The main hypothesis to explain the observed changes is  
100 a modification of the quality and/or quantity of sardine preys (such as copepods, ~~(Brosset et al., 2016)~~  
101 due to ~~major-multifactorial~~ environmental changes (SST, Upwelling, Stratification, Convection, WeMO,  
102 Chla concentration etc. Feuilleley et al., 2020), thus limiting fish energy resources (bottom-up control,  
103 Brosset et al., 2016; ~~Feuilleley et al., 2020~~; Saraux et al., 2019). However, little is known about a potential  
104 impact of contaminants on Mediterranean sardines, as few ecotoxicological studies have been performed  
105 so far on small pelagic fishes in the Gulf of Lions (but see COSTAS project; Tronczynski et al., 2013 and  
106 SUCHIMED campaign; Bouchoucha 2021). In the Mediterranean Sea, surface-enriched concentrations of  
107 multiple metals (Co, Cu, Ni and Zn), along with their significant negative correlation with salinity, suggest  
108 that concentrations are influenced by the Rhône River plume (e.g. Cossa et al., 2017; Radakovitch et al.,  
109 2008). Without a significant tide, the surface extension and main direction of this plume depend on wind  
110 and outflow forcing conditions (Broche et al., 1998). In addition, given the sardines' considerable  
111 swimming ability, it is uncertain how the spatial distribution of pollutants can overlap that of sardines.  
112 Hence, it is crucial to obtain a thorough knowledge of the contamination pressures exerted on small  
113 pelagic species such as sardines, as already highlighted by the United Nations Environment Programme  
114 UNEP (Baker et al., 2013).

115 The present study therefore focused on assessing in-situ trace element contamination in juvenile  
116 European sardines in the Gulf of Lions (NW Mediterranean Sea) and on the impact of contaminant  
117 cocktails on individual health using a proteomic approach. The specific objectives of this work were to: (i)  
118 assess the trace element load in wild juvenile sardines and evaluate the spatial variability of this  
119 contamination; (ii) investigate the impact of trace element mixtures on the proteome of liver (the main  
120 organ implicated in xenobiotic metabolism as well as blood glucose regulation, protein synthesis, bile  
121 production, vitamin and mineral storage, steroid metabolism, and immune function~~the metabolism of~~  
122 xenobiotics) and red muscle (an organ with high metabolic capacity contributing to a major part of total  
123 muscle respiration rate, see Teulier et al., 2019), and identify potential new biomarkers for both tissues  
124 that could serve as valuable tools in the long-term monitoring of European sardines' health.  
125

## 126 **Methods**

### 127 **Study sites and sampling**

128 We collected 105 juvenile sardines in the Gulf of Lions (northwestern Mediterranean Sea, Figure 1).  
129 Specimens were collected in June-July 2021 during the yearly PELMED pelagic survey conducted by the  
130 French Institute for the Exploitation of the Sea (Bourdeix & Hattab, 1985). Trawl locations were  
131 dependent on the acoustic echoes detected but covered a wide west-east gradient. Between 3 to 12  
132 sardines per trawl were selected. Sagittal otolith pairs were removed from their otic cavity and read to  
133 estimate age. Only age 0 individuals were selected for further analyses. All individuals were measured  
134 (total length TL, in mm) using a metal ruler ( $\pm 0.1\text{mm}$ ) and weighed (total mass M, in g) using a digital  
135 balance ( $\pm 1\text{g}$ ). Their body condition was calculated using the Le Cren index Kn as estimated by Brosset et  
136 al., (2015), which is commonly used as an indicator of general well-being:

$$Kn = \frac{WW}{0.00607 \times TL^{3.057}}$$

137 where WW is the total wet mass in g and TL the total length in cm.

138

139

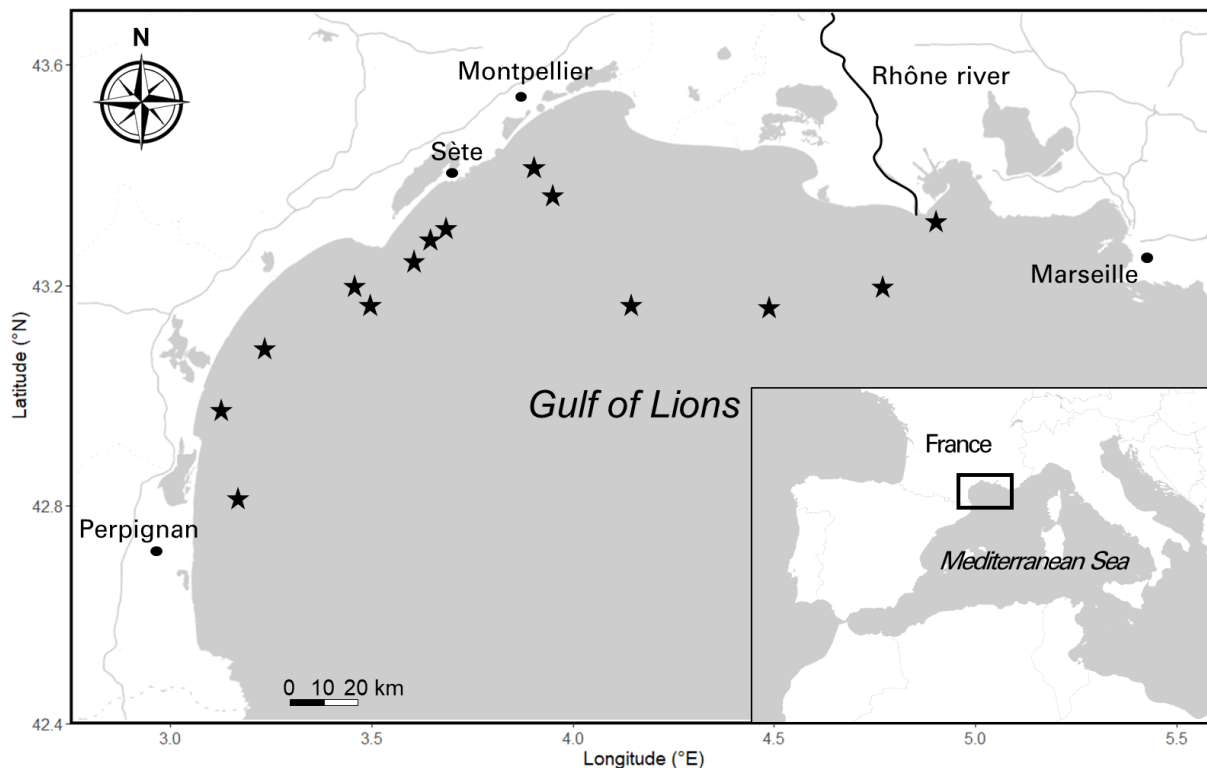


**Figure 1.** Study area in the Gulf of Lions (northwestern Mediterranean Sea). Pelagic trawling locations for the 105 *S. pilchardus* juveniles in the Gulf are indicated by (★).

140 Liver and a piece of red muscle were carefully removed to avoid any protein contamination  
 141 (gloves, a hairnet and a mask were worn by the experimenter and ceramic tools washed with ethanol 96°  
 142 and MilliQ water), immediately frozen in a dry shipper containing liquid nitrogen (~-190°C, ©CX100  
 143 Worthington Industries) on-board and later stored at -80 °C at the lab until proteomics analyses. The  
 144 white muscle on both sides of the fish was removed using cleansed ceramic tools to avoid any metal  
 145 contamination and stored at -40°C on-board for the week at sea and then stored at -80°C at the lab until  
 146 trace element analyses (one side) and lipid content (other side). The red muscle was cleanly separated  
 147 from the white muscle by scraping the lateral skin stripped from the animal. White muscle samples were  
 148 taken from the epaxial mass.

#### 149 **Body condition and reserve lipids**

150 Fish body condition was further investigated by determining white muscle reserve lipid content.  
 151 Lipids were extracted using roughly 0.1 g of muscle in a solvent mixture of chloroform-metahnom 2 : 1,  
 152 v/v according to the method of Folch et al., (1957) and the content of each class of lipids was measured  
 153 by chromatography, using a latroscan as detailed in Sardenne et al., (2019). Triacylglycerols (TAG),  
 154 diacylglycerols (DAG as TAG precursors) and free fatty acids (FFA) were grouped together as reserve lipids  
 155 (Zhol et al., 1995; Tocher 2003; Lloret et al., 2013). The proportions of free fatty acids (FFA) were also  
 156 checked to ensure that the lipids had not been degraded during sample storage. Here, the proportions  
 157 were 0.02% on average (only one sample exhibited a concentration in FFA, whereas all the others  
 158 showed no presence of FFA), significantly below the 25% limit recommended by Parrish (1988).  
 159

#### 160 **Trace-element analysis**

161 All samples were lyophilized using a freeze dryer (®Leybold, Cologne, Germany). For aluminium (Al),  
 162 arsenic (As), beryllium (Be), bismuth (Bi), cadmium (Cd), chromium (Cr), copper (Cu), lithium (Li), nickel  
 163 (Ni), lead (Pb), rubidium (Rb), antimony (Sb), strontium (Sr), titanium (Ti), thallium (Tl) and zinc (Zn)  
 164 determination, the samples underwent a pre-treatment process where 0.5 grams of each muscle sample  
 165 were subjected to acid digestion using 4 mL of HNO<sub>3</sub> (69%) and 1 mL of H<sub>2</sub>O<sub>2</sub> (33%) in special Teflon  
 166 reaction tubes within a microwave digestion system (UltraClave-Microwave Milestone®) for 20 minutes  
 167 at 220 °C, and then diluted to 10 mL with double deionized water (Milli-Q). Samples were analyzed using

168 inductively coupled plasma optical emission spectrometry (ICP-OES, ICAP 6500 Duo, Thermo) to  
169 determine the levels of these elements. The detection limit was 0.001 mg/kg. Each sample was read in  
170 duplicate and averaged. Based on UNE-EN ISO reference 11885, multi-element calibration standards (SCP  
171 Science, in 4% nitric acid) were assembled with different concentrations of inorganic elements. For  
172 calibration, see (Romero et al., 2020).

173 Total mercury (Hg) content was measured using an atomic absorption spectrometer AMA254  
174 Advanced Mercury Analyzer (Leco) without pre-treating or pre-concentrating the samples (wavelength =  
175 253.65 nm, detection limit (DL) = 0.003  $\mu\text{g}\cdot\text{g}^{-1}$ ). The recovery rate for reference materials (Mercury ICP  
176 Standard 1000  $\text{mg L}^{-1}$  Hg, Merck) was above 95%.

177

### 178 **Quantitative proteomic analysis**

179 In the following proteomic approach, we opted to analyze a subset of 29 individuals who  
180 exhibited the most distinct contamination profiles. This selection process involved assigning ranks to  
181 sardines based on the level of each contaminant detected. The ranking ranged from 1 (indicating the  
182 lowest contamination level) to 105 (representing the highest contamination level). The individuals were  
183 then selected based on the total sum of these ranks. Consequently, we identified two groups, one  
184 comprising 14 sardines with the lowest contamination levels, and the other consisting of 15 sardines with  
185 the highest contamination levels (see Statistical analysis section for further details on individuals’  
186 selection). Proteomic analyses of liver and red muscle were conducted as two separate experiments. The  
187 process of sample preparation, nanoLC-MS/MS analysis, and mass spectrometry data analysis is  
188 described in detail in ESM1. The procedure involved protein extraction and electrophoresis using SDS-  
189 PAGE, followed by in-gel digestion with trypsin (Promega, Madison, WI, USA). The resulting peptides  
190 were extracted and analyzed using a nanoUPLC-system (nano-Acquity, Waters, Milford, MA, USA)  
191 coupled to a quadrupole-Orbitrap hybrid mass spectrometer (Q-Exactive HF-X, Thermo Scientific, San  
192 Jose, CA, USA), controlled by XCalibur software (v4.0.27.9; Thermo Fisher Scientific). The Q-Exactive HF-X  
193 was operated using a data-dependent acquisition (DDA) strategy by selecting the Top-20 most intense  
194 ions in MS1 for fragmentation in MS2. MS raw data processing was performed in MaxQuant (v2.0.3.1)  
195 (Cox et al., 2014), using Andromeda algorithm to search peaklists against a protein database containing  
196 protein sequences from a home-made annotation of the genome of [the European sardine \*Sardina\*](#)  
197 [pilchardus](#) (TaxID: 27697; Genbank assembly accession: GCA\_003604335.1; Assembly Name: UP\_Spi).  
198 Only the proteins identified with at least two peptides were retained. Protein quantification was  
199 performed using unique peptides only via the MaxLFQ option implemented in MaxQuant (Cox et al.,  
200 2014) [which is a label-free quantification \(LFQ\) method that determines protein abundance based on the](#)  
201 [intensity of peptide signals](#). The mass spectrometry proteomics data have been deposited to the  
202 ProteomeXchange Consortium via the PRIDE (Perez-Riverol et al., 2019) partner repository with the  
203 dataset identifiers PXD037276 (liver) and PXD037313 (red muscle). QC-related measurements indicated  
204 stable performances of the analysis system all along the two experiments, with median coefficients of  
205 variation (CV) of 0.47% (liver) and 0.56% (red muscle) for retention times of iRT peptides over all  
206 injections. Median CVs of only 10.9% (liver) and 13.8% (red muscle) were obtained for LFQ values of the  
207 proteins quantified from the repeated injections of reference samples.

208

### 209 **Protein functional annotation**

210 To analyse our proteomic data from a functional point of view, we examined the functional  
211 annotations of proteins listed by the AMIGO consortium (Gene Ontology, GO; <http://geneontology.org/>).  
212 However, only one [S. pilchardus sardine](#) protein is annotated in GO databases. We therefore took  
213 advantage of the crucial evolutionary position of the spotted gar (*Lepisosteus oculatus*) between teleost  
214 fishes and humans, which creates a very valuable bridge between their genomes (Braasch et al., 2016),  
215 and of the fact that gar proteins are well annotated in GO databases. We began by searching *L. oculatus*  
216 sequences (UniprotKB, 22,463 protein entries; September 2022) for proteins homologous to *S. pilchardus*  
217 proteins using BLAST searches (FASTA v36.1.4 program; downloaded from  
218 [http://fasta.bioch.virginia.edu/fasta\\_www2/fasta\\_down.shtml](http://fasta.bioch.virginia.edu/fasta_www2/fasta_down.shtml)), and only the top BLAST hit for each  
219 protein was retained. From *L. oculatus* protein sequences, the same strategy was employed to search for  
220 human homologous proteins (TaxID: 9606; Reference proteome accessed in September 2022). The  
221 relevance of the match between homologous proteins was checked manually and only 57 of 2505 and 22

222 of 1112 matches (liver and red muscle, respectively) could not be validated. An automatic extraction of  
223 GO annotations was then performed using the MSDA software (Carapito et al., 2014).

224

## 225 **Statistical analyses**

226 All statistical analyses were performed with the statistical open source R software v.4.1.1 ((R Core  
227 Team, 2021). Element concentrations below Limit Of Detection (LOD, 0.001 mg/kg) were set to "LOD/ $\sqrt{2}$ "  
228 as suggested by Verbovsek (2011) as the best substitution method.

229 Analyses comparing inorganic contamination patterns included only metals that were detected in at  
230 least 50% of individuals out of the 105 collected. In order to consider possible relationships between  
231 contamination and fish body size, we used a linear model (LM) between each contaminant concentration  
232 and the individual total length. Normality and homoscedasticity of the residuals were verified using the  
233 Shapiro's and Levene's tests, respectively. When distribution of the residuals did not follow a normal  
234 distribution, a log transformation was applied prior to model fitting. If necessary ( $P < 0.05$ ), size-corrected  
235 contaminant was defined as back-transformed residuals of the regression model.

236 To investigate relationships between contaminants and to evaluate a possible influence of the Rhône  
237 River on trace element loads in sardines within the Gulf of Lions, we performed a Principal Component  
238 Analysis (PCA) on scaled size-corrected contaminant concentrations of the 105 individuals and projected  
239 distance from the Rhône River on the PCA. We also assessed spearman correlation between the three  
240 first principal components (PCs) and the distance of the individuals from the Rhône River delta. To  
241 evaluate a potential effect of inorganic contamination on individual's condition, we also performed LMs  
242 between the first three PCs and body condition and reserve lipids.

243 A second PCA approach was performed, using the 29 individuals selected for proteomic analysis as  
244 objects only, while the descriptors were scaled size-corrected contaminant concentrations. The aim of  
245 this analysis was to summarize all the information to investigate the relationships between contaminants  
246 and individual proteomes. PCA axes (PC1, PC2, PC3) were retained as principal components reflecting  
247 contaminant mixture 1, mixture 2, mixture 3 and used in further analyses.

248 Prior to statistical analyses, the proteomic datasets (liver and red muscle) were filtered to keep only  
249 proteins that were expressed in at least 70% of individuals in each contamination group (common  
250 threshold used in existing literature (Quque et al., 2023; Wang et al., 2020) leaving 2115 (out of 2505)  
251 and 913 (out of 1112) expressed proteins in the liver and red muscle, respectively. Three and one  
252 individuals were removed due to a high number of missing values for liver and muscle proteome analysis,  
253 respectively (supported by the missing value heatmap and proteomic clustering isolation of these  
254 individuals). Remaining missing values were imputed for each contamination group based on random  
255 forest method (Jin et al., 2021; Kokla et al., 2019). Previous studies have shown that this method exhibits  
256 strong performance and is particularly well-suited for label-free proteomic studies, where the underlying  
257 reasons for missing data are not fully understood (Jin et al., 2021; Kokla et al., 2019). A log 2  
258 transformation was used to normalize the protein intensities.

259

## 260 **Co-expression network and enrichment analysis**

### 261 *Gene co-expression network and hubproteins identification*

262 Weighted gene co-expression network analysis implemented in the WGCNA R package  
263 (Langfelder & Horvath, 2008) was used for both tissues (liver and red muscle) to identify groups, or  
264 modules, of proteins whose expression significantly correlates with inorganic contamination in white  
265 muscle. First, an adjacency matrix for all pairs of proteins was constructed using the Spearman  
266 correlation raised to the power (beta) of seven and six to approximate a scale-free network for liver and  
267 red muscle, respectively (Langfelder & Horvath, 2008). The adjacency matrix was then transformed into a  
268 topological overlap dissimilarity matrix and a combination of hierarchical clustering and a dynamic tree-  
269 cutting algorithm were used to first define and then merge co-expressed modules of proteins. Proteins  
270 outside any module (indicating low co-expression) were gathered in a grey module. The module's  
271 eigengene (i.e. first module eigenvector: first axis of a principal component analysis conducted on the  
272 expression of all module proteins) summarizes the expression of all proteins in that module. Then, we  
273 investigated whether the eigengene of the modules was correlated with each contaminant mixture  
274 (identified through the PCA analysis, see above), using spearman correlation. Modules with a significant  
275 ( $P < 0.05$ ) correlation and at least  $R \geq 0.4$  were retained for further analysis (only the grey module

276 (indicating low co-expression) for muscle presented a significant correlation below 0.4). Positive and  
277 negative relationships reflect the up- and down-regulation of the module with an increasing  
278 concentration of a contaminant mixture, respectively. To explore the functional and physiological  
279 mechanisms associated with each module, we then performed functional enrichment analyses.

#### 280 *Functional enrichment analysis and pathway network*

281 For both tissues, enrichment analysis (biological process and cellular component) of the proteins  
282 constituting each module was performed using Fisher's exact test using the 'GO\_MWU' package  
283 particularly suitable for non-model organisms ([https://github.com/z0on/GO\\_MWU](https://github.com/z0on/GO_MWU)) (Dixon et al., 2015).  
284 The background used for each tissue consisted of the set of proteins identified in that specific tissue,  
285 ensuring two distinct backgrounds for the analysis. This approach prevents biased enrichment from a  
286 generic background, ensuring accurate determination of the functional significance of the identified  
287 modules (Wijesooriya et al., 2022). ~~It allows to determine the functional significance of the identified~~  
288 ~~modules~~. Enriched GO terms are displayed in a dendrogram plot with distances between terms reflecting  
289 the number of shared proteins. Additionally, we assessed the Spearman correlation between each  
290 protein and the contamination mixtures (PCA axes) to infer "gene significance" (GS). Focusing on the top  
291 10 enriched biological process terms (GO terms), these GS relationships were compiled within a circle  
292 plot for each enriched pathway of the module. These plots highlight the up- or down-regulation of the  
293 proteins and pathways in response to the contaminant mixtures.

294

#### 295 *Network visualization*

296 ClueGO was used to illustrate overrepresented Gene Ontology terms. ClueGO is a Cytoscape  
297 plug-in that visualizes the non-redundant biological terms for large numbers of proteins and integrates  
298 the GO terms to create a GO/pathway network (Bindea et al., 2009). A network for each tissue was made  
299 in order to visualize the pathways impacted by the three contamination mixtures.

300

#### 301 *Hubproteins identification*

302 For each module, GS was correlated with module membership (MM; spearman correlation of  
303 protein intensity versus the module eigengene) to identify proteins showing the highest degree of  
304 connectivity within a module and with the considered contaminant mixture (hubproteins). The top 5  
305 proteins with simultaneously the highest MM and GS (rank sum) were selected as hubproteins in each  
306 module. Due to their central position in the network, hubproteins are expected to play important  
307 biological roles within their module and are considered as potential biomarkers.

308

#### 309 *Functional Comparison between tissues*

310 For each contamination mixture, the similarity of the functional response between tissues was  
311 compared by plotting their respective GO term delta ranks against each other. GO term delta ranks  
312 correspond to the difference between the mean ranks based on the GS of the proteins the GO term  
313 contains vs the mean ranks of all the protein not included. Positive and negative delta ranks indicate that  
314 the GO term tends to be regulated upwards or downwards, respectively. For a given pathway, the  
315 strength of the relationship reflects the similarity of the enrichment between liver and red muscle. It is  
316 important to note that these plots do not represent a formal statistical test, as the data points (gene  
317 ontology categories) are not independent. Indeed, they often encompass overlapping sets of proteins,  
318 nonetheless it allows identifying functional similarity or dissimilarity between functional enrichments.

319

320

## Results

321

### 322 **Trace-element burden across Gulf of Lions**

323

324 Thirteen trace elements (Al, As, Cu, Cr, Hg, Li, Ni, Pb, Rb, Sr, Ti, Tl and Zn, ESM2) were retained  
325 after selection of contaminants detected (>LOD) in at least 50% of individuals (i.e. 53 individuals). Only  
three elements (Pb, Rb and Tl) exhibited a significant relationship with fish length and were size-

326 corrected. While Tl displayed a negative relationship with length ( $R^2 = 0.16$ ,  $P < 0.001$ ), Pb and Rb had a  
327 positive association ( $R^2 = 0.10$ ,  $P = 0.009$  and  $R^2 = 0.09$ ,  $P = 0.001$  respectively).

328 Considering the 105 sardines sampled across the Gulf of Lions within the same PCA, the first three  
329 principal components explained 24.2%, 15.3% and 12.8%, respectively (around 52% in total, ESM3a and  
330 Figure 2). The main contributing variables for the first axis (PC1) were Zn, Sr, Rb, Cu, Pb and As, which all  
331 displayed positive contributions (ESM3b and Figure 2). Ni, Cr were positively related to PC2 while, to a  
332 lesser extent, Tl was negatively loaded (ESM3c and Figure 2). Ti and Al were negatively loaded along the  
333 third axis in opposition to Cr, Ni, Tl and Li (ESM3d and Figure 2). Highlighting the distance of the various  
334 sampling sites to the mouth of the Rhône River within the same PCA showed a slight east-west  
335 contamination gradient (Figure 2). PC1 and PC2 were negatively correlated with the distance from the  
336 Rhone river, albeit slightly above significance levels (ESM4). Nonetheless, there was considerable inter-  
337 individual variability in trace element contamination, which probably blurred this East-West gradient  
338 (ESM4). The three first PCs displayed no significant correlation with individuals' body condition ( $P = 0.47$ ,  
339  $P = 0.18$  and  $P = 0.57$  for PC1, PC2 and PC3 respectively), nor with the reserve lipid content ( $P = 0.55$ ,  
340  $P = 0.66$  and  $P = 0.79$  for PC1, PC2 and PC3 respectively).

341

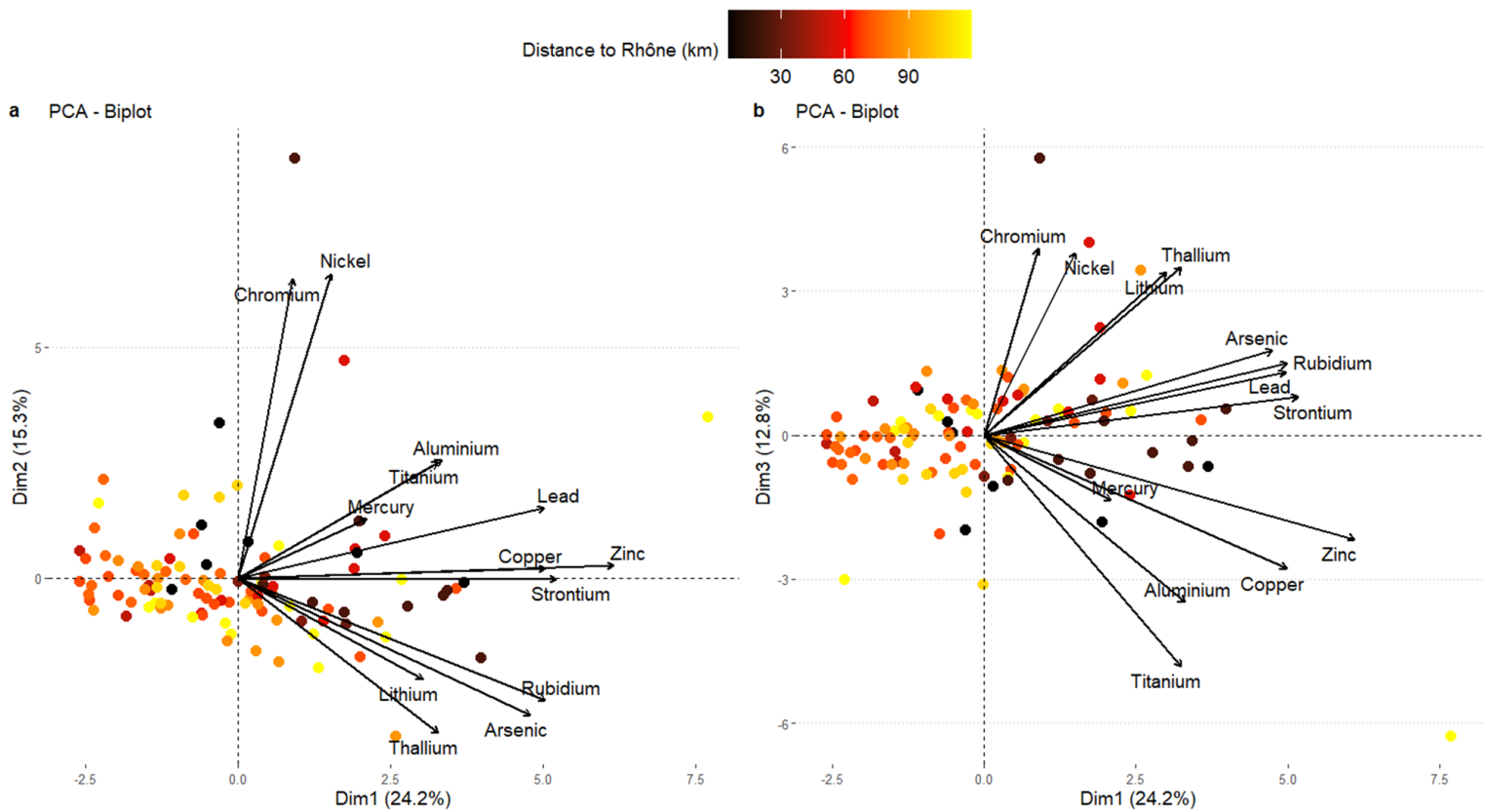


**Figure 2.** Biplot of PC1 vs PC2 (a) and PC1 vs PC3 (b) of the PCA built with size-corrected level of trace elements present in the 105 individuals sampled across the Gulf of Lions. Each point represents an individual. Colour gradient indicates the distance from the Rhone river.

342 Regarding the second PCA performed on the 29 individuals selected for proteomic analysis, the first  
343 three principal components displayed 33.3%, 16.9% and 13.6% of the total variance, respectively (around  
344 64% in total, Figure 3 and ESM5). All 13 contaminants loaded positively on PC1 with 8 of them  
345 contributing strongly. Further, PC1 clearly separated the 2 groups of individuals previously selected (high  
346 contamination vs low contamination). Therefore, PC1 was used as a proxy for general inorganic  
347 contamination level, which allows to work along a contamination gradient instead of categorical  
348 contaminations. PC2 was mostly determined by a strong positive contribution of Ni and Cr, while PC3 was  
349 determined by a strong positive contribution of Ti and Al and marginally by a negative contribution of Li.



350 The three PCs independently identified contaminant mixtures, which are listed in Table 1. We next used  
 351 proteomics to investigate the potential impact of these three contaminant mixtures on the health of the  
 352 Mediterranean sardine population.

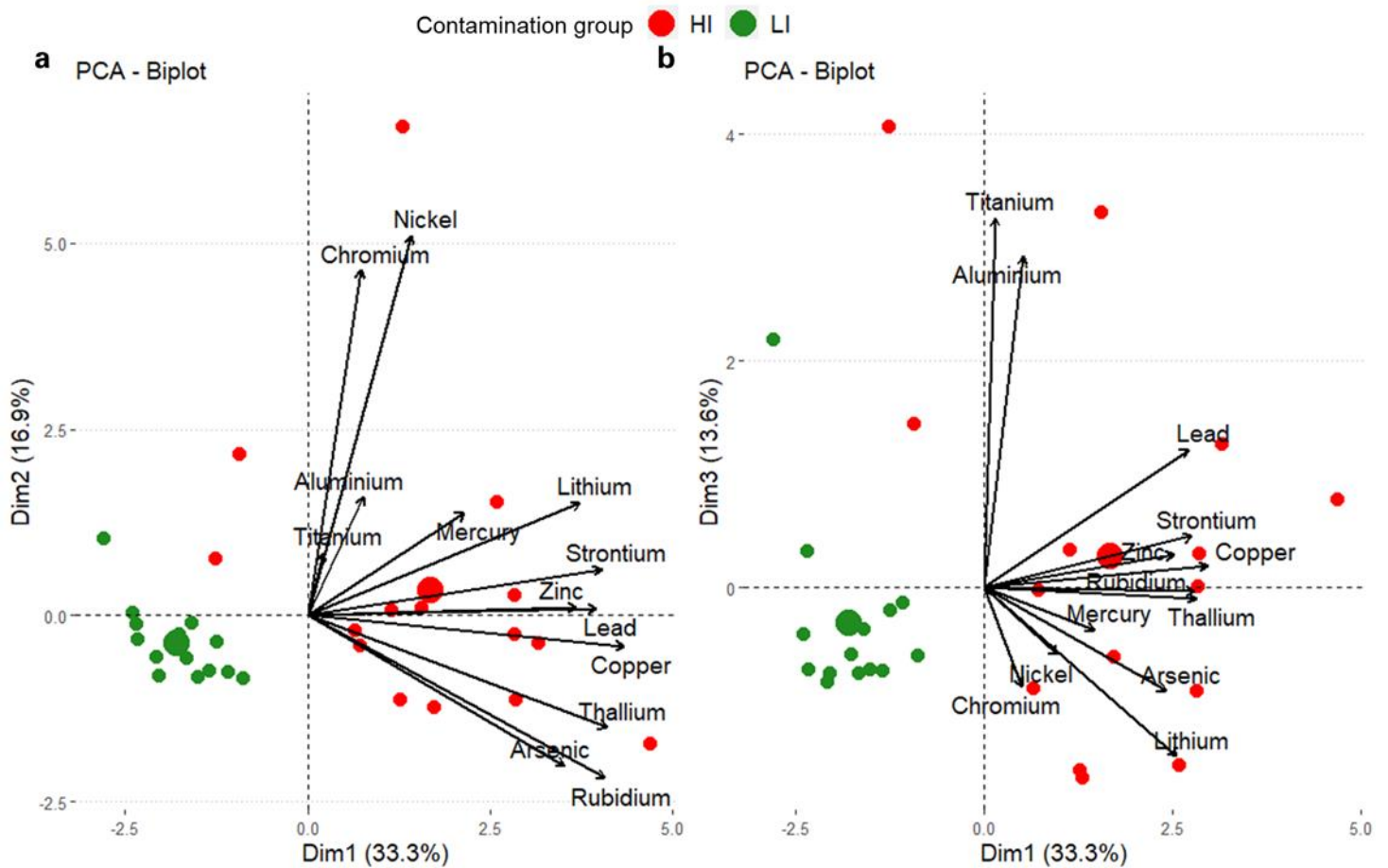


**Figure 3.** Biplot of PC1 vs PC2 (a) and PC1 vs PC3 (b) of the PCA built with level of inorganic contaminants present in the 29 individuals selected for proteomic analysis. Each point represents an individual. Colours indicate contamination level of individuals (HI: High contamination and LI: Low contamination). The larger circles represent the barycenter of the individuals for a given group.

353

354 **Table 1.** Main variables that contribute to the first three principal components of the PCA on the 29 individuals selected for  
 355 proteomic analysis. Each PC represents a contaminant mixture.

Mixture 1 - PC1		Mixture 2 - PC2		Mixture 3 - PC3	
-	+	-	+	-	+
none	Cu, Tl, Rb, Sr, Pb, Li, Zn, As	none	Ni, Cr	Li	Ti, Al

356

### 357 **Physiological response to inorganic contamination**

358 Using a co-expression network analysis, we focused on the impact of metal contamination at the  
 359 proteome level on two key organs in fish (the liver and red muscle).

#### 360 *Liver proteome*

361 We detected 9 distinct modules (WGCNA analysis) containing a total of 2115 proteins. We then  
 362 investigated the relationship between expression modules and the three metal contamination mixtures  
 363 to assess the potential health effects of inorganic contaminant exposure. Both mixtures 1 and 3 displayed

364 | significant positive correlations ( $P < 0.05$ , encompassing approximately 31% of the detected proteins) with  
 365 | the same two co-expressed modules (turquoise and yellow, Figure 4), reflecting a general overexpression  
 366 | of proteins within these 2 modules when mixtures 1 and 3 increased in concentration. Mixture 2 did not  
 367 | display any relationship with any of the co-expressed modules.

	turquoise (453)	yellow (201)	brown (218)	green (181)	red (133)	pink (107)	black (127)	blue (426)	grey (269)
Mixture 1	0.52 **	0.6 **							
Mixture 2									
Mixture 3	0.46 *	0.6 **							

**Figure 4.** Correlations between module eigengenes (columns) and trace element mixtures (rows) for liver proteome. Values in brackets with module names indicate the number of proteins belonging to each module. Values in the cells are Spearman's correlation coefficients. Blank cells indicate non-significant correlation ( $P > 0.05$ ). \*:  $P < 0.05$ , \*\*:  $P < 0.01$

368 | The positive correlation of the turquoise module with mixture 1 (PC1,  $r = 0.52$ ,  $P < 0.01$ ) and mixture 3  
 369 | (PC3,  $r = 0.46$ ,  $P < 0.05$ ) involved an overall upregulation of 170 GO terms ( $FDR < 0.01$ ), mainly involved in  
 370 | anatomical structure and development (e.g., epithelial cell development (GO:0002064), regulation of  
 371 | anatomical structure size (GO:0090066)), response to stimulus/stress (e.g. defense response  
 372 | (GO:0006952), cellular response to DNA damage stimulus (GO:0006974)), protein metabolism (e.g.  
 373 | positive regulation of gene expression (GO:0010628), regulation of protein polymerization), transport  
 374 | and cellular organization (e.g. cell development, regulation of cytoskeleton organization) and cell cycle  
 375 | process (spindle organization, cell cycle process, Figure 5 and ESM6a). Proteins from the turquoise  
 376 | module were part of multiple subcellular compartments, such as the nuclear periphery, endocytic  
 377 | vesicles, immunological synapses and the cytoskeleton (ESM6b). The positive correlation of the yellow  
 378 | module with mixture 1 ( $P < 0.001$ ) displayed a significant enrichment in 71 pathways mainly related to the  
 379 | immune system, the metabolism of lipids and lipoproteins and transport (Figure 5 and ESM7a). Most of  
 380 | these pathways were upregulated in response to an increase in mixture 1 (i.e. Cu, Rb, Sr, Tl, Zn, Li, Pb and  
 381 | As). As for the cellular component analysis, proteins were mainly located in lumens (vesicle, endoplasmic,  
 382 | endocytic) and were subunits of protein complexes (protein-lipid complex, hemoglobin complex, ESM7b).

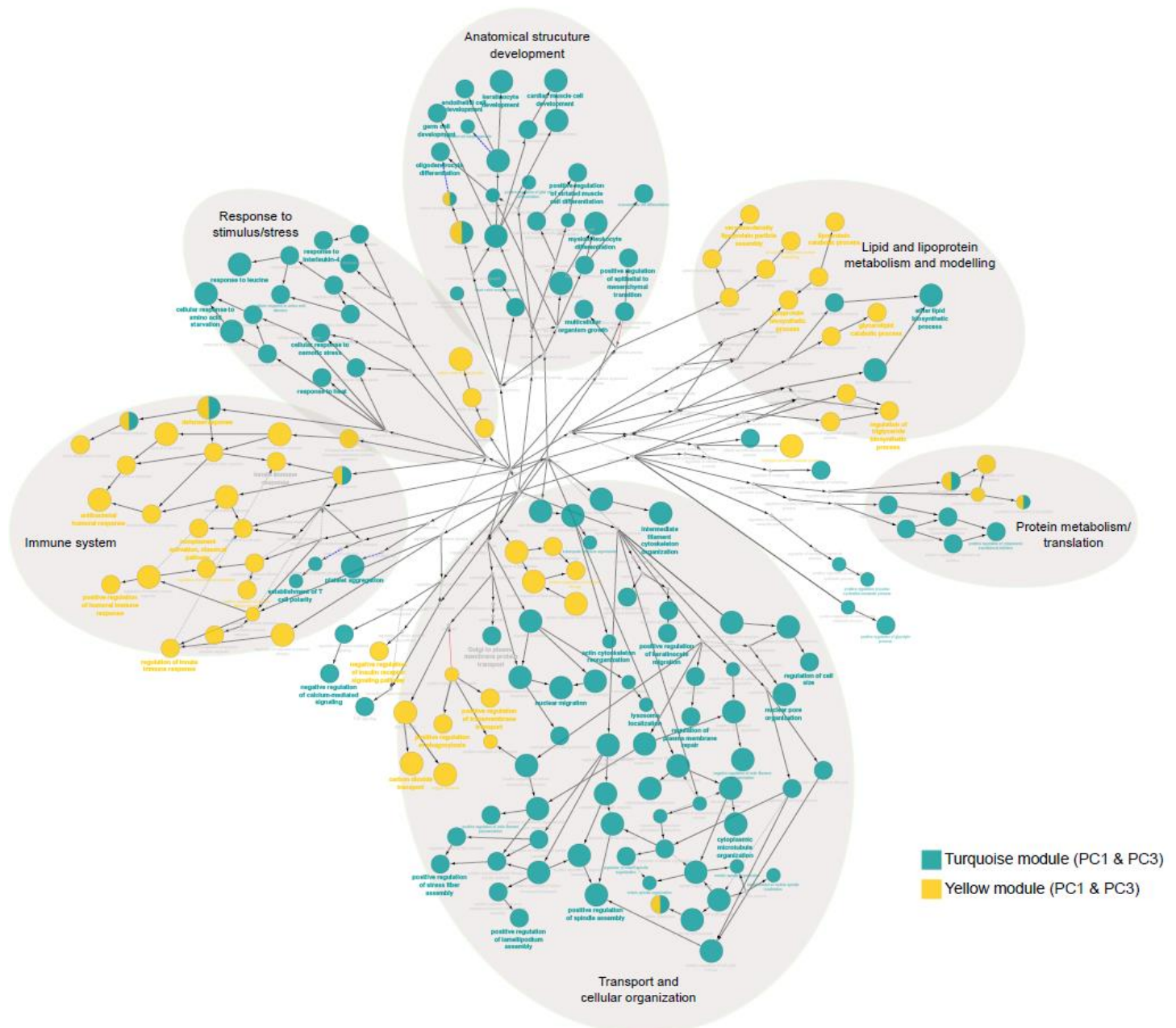


**Figure 5.** Significant GO terms (FDR < 0.001) and ontological relationships in the liver. Colored circle size reflects the level of FDR-adjusted statistical significance. Terms enriched in the same module were grouped and presented in the same color. Each leading term, which has the highest significance, is indicated by bold font. Biological processes were grouped in larger pathways (large grey circles).

383 To identify potential biomarkers, hubproteins (top 5 proteins with the highest GS and MM) were  
 384 selected for each module (see Table 2). For the turquoise module, hubproteins were mainly implicated in  
 385 protein or lipid transport (Table 2). Interestingly, one of them, the Serine/threonine- protein kinase  
 386 mTOR, was involved in multiple pathways such as cell development, cell structure and metabolism.  
 387 Potential biomarkers for the yellow module included 2 apolipoproteins with one presenting antioxidant  
 388 activity (i.e., the Apolipoprotein A-IV). The three other hubproteins were involved in diverse pathways  
 389 such as protein synthesis with the eukaryotic translation initiation factor 2 subunit 3, cytoskeleton and  
 390 protein transport with the spectrin beta chain and the DnaJ homolog subfamily C member 13 which is not  
 391 only implicated in protein transport but also exhibits chaperon function.

**Table 2.** Top 5 hubproteins selected for each co-expression module in the liver proteome. The name and UniprotKB ID are indicated for each of them as well as their main functions, their module, their expression pattern (up or down-regulation), contaminant mixture they correlate with and the module membership

Name	UniprotKB ID	Module	Main function	Expression pattern	Principal Component	Module membership
Apolipoprotein B-100 isoform 3	APOB	turquoise	Lipid transport and metabolism	↑ up	PC1 and PC3	0.83
Serine/threonine-protein kinase mTOR	MTOR	turquoise	Cell growth, Cell cycle progression, Metabolism, Cellular structure	↑ up	PC1 and PC3	0.81
Cytoplasmic dynein 1 heavy chain 1 isoform 5	DYNC1H1	turquoise	Intracellular motility: cell cycle and transport	↑ up	PC1 and PC3	0.78
U5 small nuclear ribonucleoprotein 200 kDa helicase	SNRNP200	turquoise	mRNA processing/splicing	↑ up	PC1 and PC3	0.89
Cytoplasmic dynein 1 heavy chain 1 isoform 2	DYNC1H1	turquoise	Intracellular motility: cell cycle and transport	↑ up	PC1 and PC3	0.80
Apolipoprotein A-IV	APOA4	yellow	Lipid transport and metabolism, Antioxidant capacity	↑ up	PC1 and PC3	0.88
Apolipoprotein B-100 isoform 1	APOB	yellow	Lipid transport and metabolism	↑ up	PC1 and PC3	0.79
Eukaryotic translation initiation factor 2 subunit 3	EIF2S3	yellow	Translation	↓ down	PC1 and PC3	-0.77
Spectrin beta chain, non-erythrocytic 1	SPTBN1	yellow	Cellular structure, Protein transport/localization	↑ up	PC1 and PC3	0.84
DnaJ homolog subfamily C member 13	DNAJC13	yellow	Chaperone, Protein transport	↑ up	PC1 and PC3	0.88

392

393 *Muscle proteome*

394 The WGCNA analysis of the red muscle proteome, containing 913 proteins, resulted in four modules  
 395 namely blue (372 proteins), brown (119 proteins), turquoise (398 proteins), and grey (24 proteins).  
 396 ~~Four modules, namely blue (372 proteins), brown (119 proteins), turquoise (398 proteins) and grey (24~~  
 397 ~~proteins), were obtained from the WGCNA analysis of the red muscle proteome.~~  
 398

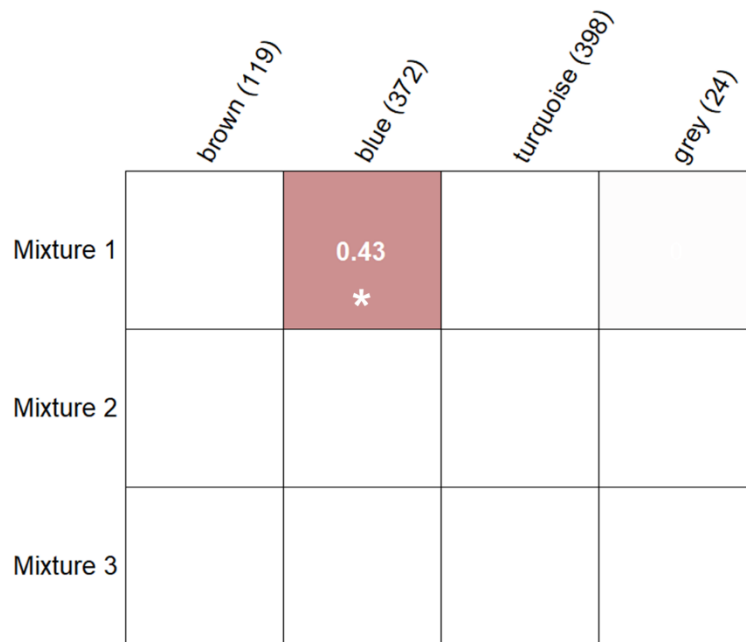


**Figure 6.** Correlations between module eigengenes (columns) and trace element mixtures (rows) for the red muscle proteome. Values in brackets with module names indicate the number of proteins belonging to each module. Values in the cells are Spearman's correlation coefficients. Blank cells indicate non-significant correlation ( $P > 0.05$ ). \*:  $P < 0.05$ , \*\*:  $P < 0.01$

399 Only the blue module, which accounts for 41% of all detected proteins in the red muscle proteome,  
 400 correlated (positively) with one contaminant mixture (i.e., mixture 1, Figure 6). This module was enriched  
 401 in cellular organization and ion transport pathways (Figure 7 and ESM8). According to the cellular  
 402 component enrichment analysis, proteins were mainly located in membranes (ESM8b).

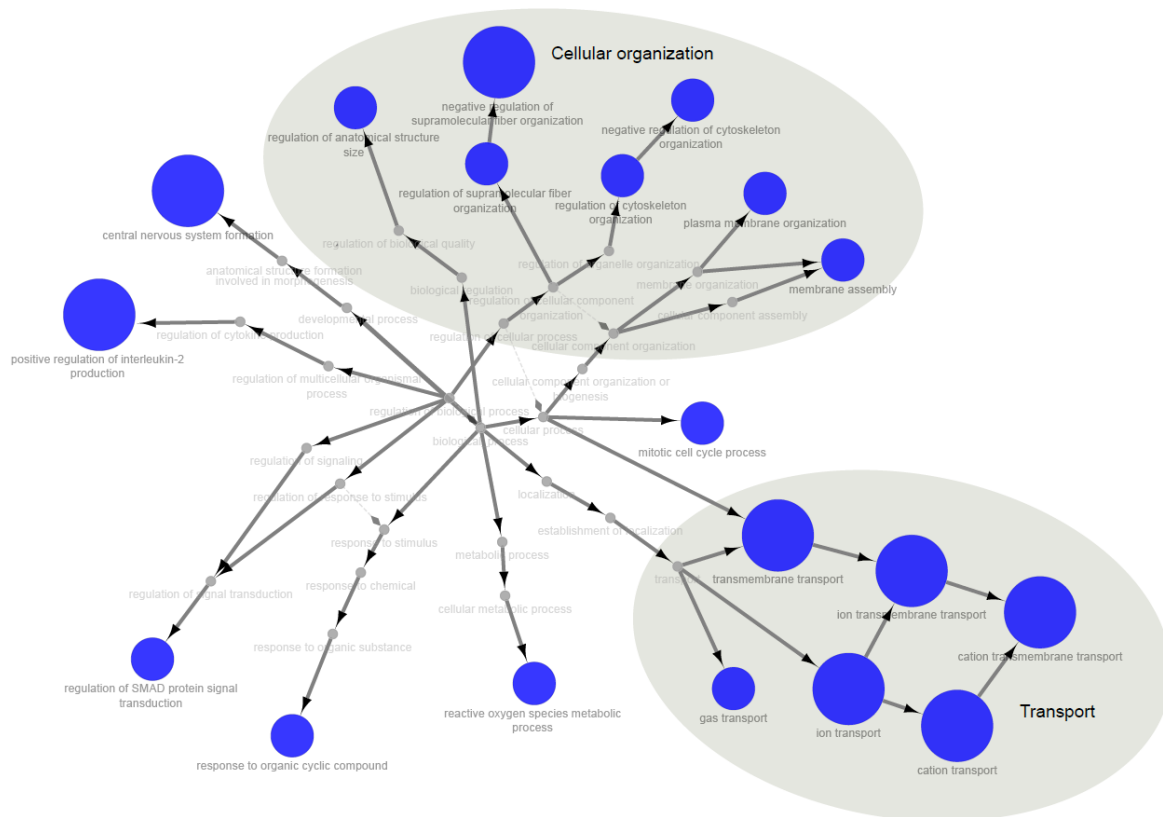


**Figure 7.** Significant GO terms (FDR <0.001) and ontological relationships in red muscle. Circle size indicates the level of FDR-adjusted statistical significance. Biological processes were grouped in larger pathways (large grey circles).

403 Two identified hubproteins for the blue module have a known function in the response to oxidative  
 404 stress (Glutathione S-transferase and Hemoglobin subunit zeta), whereas two others are involved in  
 405 cellular structure and muscle contraction (myosin-binding protein H and Myomesin-2). The last identified  
 406 hubprotein was the ADP/ATP translocase 1 which is implicated in energy metabolism and apoptotic  
 407 signaling pathway (Table 3).

**Table 3.** Top 5 hubproteins selected for each co-expression module in the red muscle proteome. The name and UniprotKB ID are indicated for each of them as well as their main functions, their module, their expression pattern (up or down-regulation), contaminant mixture they correlate with and the module membership.

Name	UniprotKB ID	Module	Main function	Expression pattern	Principal Component	Module membership
Glutathione S-transferase	LANCL1	blue	Contaminant detoxification, Oxidative stress metabolism	↓ down	PC1	-0.92
Hemoglobin subunit zeta	HBZ	blue	Gas transport, Oxidative stress metabolism	↑ up	PC1	0.90
Myosin-binding protein H	MYBPH	blue	Cell adhesion, Muscle contraction	↓ down	PC1	-0.92
ADP/ATP translocase 1	SLC25A4	blue	Transmembrane transporter, Apoptotic signalling pathway	↓ down	PC1	-0.92
Myomesin-2	MYOM2	blue	Cellular organization, Muscle contraction	↓ down	PC1	-0.91

408  
 409 *Comparison of liver vs red muscle proteome response*

410 Comparison of the delta-rank values obtained from GO enrichment analysis for both tissues against  
 411 mixture 1 revealed a significant positive correlation ( $r = 0.22$ ,  $P < 0.001$  ESM9a). Liver and muscle  
 412 enrichment for mixture 2 displayed no significant correlation ( $r = 0.02$ ,  $P = 0.96$ , ESM9b), while  
 413 enrichment for mixture 3 revealed a significant but weak positive correlation between the two tissues ( $r =$

414 0.06,  $P < 0.01$ , ESM9c). This highlights that similar processes appear involved in liver and red muscle in  
415 response to contaminant mixture 1 and, to a lesser extent, mixture 3.

## 416 Discussion

417 Multiple studies have investigated the potential drivers of the drastic decrease in size, age and body  
418 condition of sardines in the Gulf of Lions since 2008 (e.g. Brosset et al., 2015, 2016, 2017; Le Bourg et al.,  
419 2015; Van Beveren et al., 2016, 2017; Feuilloley et al., 2020). However, thorough information on chemical  
420 contamination by trace elements and its physiological impact on this species was lacking. We found  
421 evidence for the accumulation of multiple elements in sardines, with a light East-West contamination  
422 gradient within the Gulf of Lions. While macro-physiological parameters (i.e. body condition) were not  
423 affected by contamination, pathways involved in cellular organization and response to stress were clearly  
424 upregulated, particularly in the liver, but also in muscle. In addition, a global upregulation in processes  
425 linked to the immune system and lipid homeostasis was recorded in the liver. We are proposing  
426 biomarkers of the effects of trace element stress on health, which could serve as a starting point in  
427 biomonitoring programs.

428

### 429 Contamination load in the Mediterranean sardine of the Gulf of Lions

430 The impact of contaminating loads from the Rhône River on the organisms living in the Gulf of Lions  
431 has already been reported with regard to radionuclides, such as  $^{210}\text{Po}$  (Strady et al., 2015), heavy metals  
432 (Cd, Pb and Hg for [60–200  $\mu\text{m}$ ] size fraction, Chouvelon et al., 2019) and organic contaminants, such as  
433 Polychlorinated biphenyls (PCBs) in plankton (Aleksenko et al., 2018). In addition to the Rhône River  
434 inputs, pollutant discharges are also likely to come from industrial and urban activities of the nearby  
435 cities of Marseille and Fos-sur-Mer. Small pelagic planktivorous fish such as sardines in the eastern areas  
436 of the Gulf of Lions might therefore be highly exposed to chemical contamination, notably via trophic  
437 pathways (i.e. plankton). Interestingly, although large inter-individual variability in contamination  
438 between individuals was recorded in our study, we noted a moderate East to West contamination  
439 gradient in the Gulf of Lions. These results differ from previous work (Chouvelon et al., 2019) that did not  
440 detect a spatial pattern in trace element contamination in the same species and location. These  
441 differences might be due to the targeted tissue, as they considered contamination in the whole organism  
442 (liver, muscle, gonad and remaining tissues) whereas we focused on muscle contamination. Indeed,  
443 factors such as tissue-specific metabolic processes, affinity for contaminants and turnover rates can  
444 contribute to distinct contamination patterns observed across different tissues. Another reason for  
445 discrepancies between our and previous studies might involve the fact that individuals were sampled at  
446 different life stages in those former studies, whereas we focused on individuals in their first year of life  
447 (age 0). Indeed, confounding effects with contaminant elimination through reproduction as well as  
448 bioaccumulation with age may explain large variations and no clear spatial pattern (Bodiguel et al., 2009).  
449 Canli and Atli (2003) highlighted the importance of fish size in determining the rate of physiological  
450 processes, as size may influence the uptake, distribution, and elimination of trace elements. In our study,  
451 only three trace elements (out of 13) displayed significant relationships with fish size, namely Pb, Rb and  
452 Tl. This lack of relationship with size for most of trace elements could result from the complexity of  
453 bioaccumulation processes involving interaction between various routes of absorption, excretion, passive  
454 release, and metabolism (Joiris et al., 1999; Guo et al., 2016; Tang et al., 2017). Yet, the study of one-  
455 year-old gilthead seabream juveniles (Beauvieux et al., 2024) showed comparable outcomes. This  
456 indicates that when examining a single age group, size differences are likely minimal, simplifying the  
457 study of spatial contamination. That said, exploring multiple age groups remains essential to uncover  
458 intricate bio-accumulation patterns.

459 Trace metal concentrations in Mediterranean surface waters and top predators are generally higher  
460 than in the Atlantic Ocean (Boyle et al., 1985; Cossa and Coquery 2005). This phenomenon can be largely  
461 attributed to the Mediterranean's semi-enclosed geography, which promotes pollutant accumulation.  
462 This accumulation is further exacerbated by significant atmospheric inputs, such as Saharan dust events,  
463 intense human activities (Bucchia et al., 2015; Pedrotti et al., 2016), and riverine discharges on  
464 continental shelves (Durrieu de Madron et al., 2011). Additionally, there is evidence suggesting that the  
465 Mediterranean pelagic food webs may have a heightened capacity to bioaccumulate certain trace

466 | [elements, particularly Hg \(Cossa and Coquery 2005; Harmelin-Vivien et al., 2009; Chauvelon et al., 2018\).](#)  
467 | [Additionally, it is suggested that ~~it could be due to the enhanced ability of the~~ Mediterranean pelagic](#)  
468 | [food ~~chains-webs~~ may have a heightened capacity](#) to bioaccumulate certain chemicals, as documented  
469 | for mercury (Cossa and Coquery 2005; Harmelin-Vivien et al., 2009; Chauvelon et al., 2018). This pattern  
470 | also turned out to be true for As, Ni, Cr, Pb, Zn and Hg in sardines recorded in numerous studies  
471 | (considering only [S. pilchardus the European sardine](#) in ESM10). Trace element concentrations found in  
472 | the present study were of a similar order of magnitude to those found in other studies focusing on the  
473 | same or close species of the Mediterranean, Atlantic or Indian Oceans, except for [lithium Li](#). Averaged Li  
474 | levels were 32 times higher than those found by Guérin et al., (2011) on the Mediterranean sardine (but  
475 | Li levels were measured in only 4 individuals in this previous work) and 2 times higher than those found  
476 | by Lozano-Bilbao et al., (2019) on [S. pilchardus the European sardine](#) in the Atlantic Ocean.

477 | Similarly to findings in seabreams (Beauvieux et al., 2024), we identified a lack of monitoring for  
478 | several elements including Li, Rb, Sr, Ti and Tl in all locations (Indian and Atlantic Oceans and the  
479 | Mediterranean Sea, ESM10 and ESM11). This is partially explained by the absence of regulatory limits for  
480 | these elements in fish muscle (along with Cr and Ni), despite their increasing use in multiple areas  
481 | (industrial, agriculture, high-tech and medication industries) and despite their toxicity for organisms  
482 | (Exley et al., 1991; Authman 2011; Aslam and Yousafzai 2017; Blewett and Leonard 2017; Kumari et al.,  
483 | 2017; Genchi et al., 2021).

484 | The European regulation sets contamination thresholds for only three specific inorganic trace  
485 | elements, Pb (~~lead~~), Cd (~~cadmium~~) and Hg (~~mercury~~). In contrast, other nations, such as Turkey and  
486 | Greece have adopted thresholds for a larger set of contaminants (for a comprehensive review, refer to  
487 | Guerra-García et al., 2023). Notably, trace element levels in sardine specimens from the present study  
488 | remained below the threshold values for fish consumption set by most international regulations except  
489 | for As that exceeded these limits. These findings emphasize the need for further efforts by the European  
490 | commission and other institutions to establish health limits not only for Arsenic but also for other  
491 | nonessential and essential elements.

492 | [Furthermore, it is important to consider the existence of organic and emerging pollutants \(POPs,](#)  
493 | [HAPs, PFOS, PFAS, etc.\) that are becoming increasingly pervasive worldwide \(Magulova & Priceputu,](#)  
494 | [2016\). Given their persistence, long-range transportability, biomagnification in food chains, and](#)  
495 | [bioaccumulation in humans and wildlife, their impact on individual health is becoming a growing concern](#)  
496 | [\(Magulova & Priceputu, 2016\). The combined effects of trace elements and POPs create a complex](#)  
497 | [chemical cocktail that can have synergistic or antagonistic impacts on marine life. Thus, there is a growing](#)  
498 | [need for additional research to fully understand the scope of contamination which requires considering](#)  
499 | [both trace elements and POPs.](#)

## 501 | **Commonly dysregulated pathways in the liver and red muscle in response to multiple-metal** 502 | **contamination**

503 | Liver and red muscle shared common proteome changes, such as cellular disorganisation as well as  
504 | functions involved in transport and stress response (Figure 5 and 7). This is in line with the positive  
505 | correlation found between the functional enrichment of the two tissues in relation to mixture 1 and  
506 | mixture 3 (ESM9), highlighting similar responses (up-regulation). However, we noted a much more  
507 | [diverse/intense](#)-response in the liver, with 17 times more pathways overexpressed compared to red  
508 | muscle. Similar results have been observed in seabreams (Beauvieux et al., 2024). This discrepancy in  
509 | responses between both tissues could be related to the liver functions, as this is the main organ  
510 | responsible for detoxification, transformation and storage of toxic compounds in fish (Bawuro et al.,  
511 | 2018; Beauvieux et al., 2024).

512 | Contaminant mixture 1 (contamination in Cu, Rb, Sr, Tl, Zn, Li, Pb and As) seemed to particularly  
513 | impact cellular organization in the two tissues, as reflected by an overexpression of multiple pathways  
514 | involved in cellular structure, intracellular transport and motility processes. In particular, two isoforms of  
515 | cytoplasmic dynein heavy chain seemed to be affected by mixture 1 in liver (along with mixture 3).  
516 | Cytoplasmic dyneins are central in intracellular trafficking, including macromolecular transport,  
517 | chromosome dynamics, and the cell cycle (Paschal et al., 1987; Kardon and Vale 2009; Bawuro et al.,  
518 | 2018). This is in line with the significant downregulation in the pathway involved in mitotic spindle  
519 | assembly that has been also detected and could indicate that trace ~~-~~element exposure has genotoxic

520 effects and may repress hepatocyte division. Similarly, cytoplasmic dyneins (Table 2) were identified in  
521 bivalves as responsive to contamination (Li & Wang, 2021; Sánchez-Marín et al., 2021), which made them  
522 great candidate biomarkers of trace element contamination. Additionally, given that proper cellular  
523 organization is crucial for organismal development, the abundance of upregulated pathways associated  
524 with anatomical structure and development may suggest a response to counteract contamination-  
525 induced disorganization. Histopathological alterations in hepatocytes have already been observed,  
526 revealing the disorganization of organelles within the cytoplasm (Moreira et al., 2003) and the presence  
527 of necrosis (Javed et al., 2017) in response to metal contamination. Since hepatocytes are involved in  
528 various aspects of intermediate metabolism, unfavourable consequences to physiology may be expected  
529 as well at the cellular and organismal level (Mela et al., 2007).

530 Red muscle proteome response to mixture 1 was displayed fewer functional diversity response less  
531 marked than that of the liver proteome, but it reflected an alteration of the biological structure of cells  
532 and, again, the cell cycle process, as highlighted by the upregulation of the pathway “mitotic cell cycle  
533 process”. Accordingly, two of the five hubproteins identified were myosin and myomesin, which are key  
534 proteins in cell adhesion and muscle contraction. This is consistent with previous works, that highlighted  
535 alterations of multiple myocytoskeleton proteins in response to contamination (Rodríguez-Ortega et al.,  
536 2003; Karim et al., 2011; Xu et al., 2019). As the contractile ability of myocytes resides in their highly  
537 organized cytoskeleton network, dysregulation here could greatly affect the locomotion of juvenile  
538 sardines, hindering their escape from predators and their foraging success.

539 The effects of trace element contamination on liver and muscle cytoskeleton are likely to be caused  
540 by oxidative stress (Epel et al., 2004), either through excess reactive oxygen species (ROS) generation (by  
541 redox-active metals) or reduction of antioxidant abundances and or activities (redox-inactive metals)  
542 (Koivula & Eeva, 2010). In this study, we highlighted the upregulation of pathways such as “cellular  
543 oxidant detoxification” and “hydrogen peroxide catabolic process” in the liver and “reactive oxygen  
544 species metabolic process” in muscle. Consequently, two potential biomarkers of red muscle proteome in  
545 response to mixture 1 were identified (down-regulated glutathione S-transferase and up-regulated  
546 hemoglobin subunit zeta, Table 3). They have both known functions in contaminant detoxification and  
547 antioxidant defences, respectively (Mollan et al., 2012). Glutathione S-transferase was underexpressed  
548 in red muscle with increasing contamination (mixture 1), suggesting a redox-inactive potential of mixture  
549 1 on this enzyme specifically but also highlighting that some canonical detoxification enzymes may be  
550 triggered or repressed by metal exposure, depending on their intrinsic nature (redox-active vs redox-  
551 inactive sensitivity).

552 Furthermore, trace element mixtures induced additional cellular responses aimed at safeguarding  
553 organisms from ROS-induced damage. Among these responses, a heat shock protein homologue (Dnaj  
554 homologue, Table 2) plays a crucial role by acting as cochaperones to the molecular chaperone (Hsp70).  
555 Its functions involve protein translation, promoting protein folding, translocation of polypeptides through  
556 membranes and degradation of damaged proteins (Mitra et al., 2009). In multicellular eukaryotes,  
557 programmed cell death, often referred to as apoptosis, is a prevalent stress response mechanism that  
558 comes into play when the level of stress surpasses the cell's ability to uphold genomic and  
559 macromolecular integrity. In this study, apoptosis signalling pathway involving ADP/ATP translocase and  
560 the serine/threonine-protein kinase mTOR (Table 3 and Table 2) appeared to be affected by trace  
561 element contamination. Previous transcriptomics and proteomics studies have reported alterations in  
562 apoptotic pathways in various fish species in response to environmental contaminants (Bohne-Kjersem et  
563 al., 2009; Leaver et al., 2010; Asker et al., 2013; Yadetie et al., 2013). The serine/threonine-protein kinase  
564 mTOR was overexpressed in response to trace element contamination in the liver, which is implicated in  
565 cellular death cascades along with lipid regulation and nutrient signaling. However, besides its  
566 abundance, post-translational modifications including phosphorylation, ubiquitination, acetylation, and  
567 glycosylation appears to be key regulators of mTOR signaling and should also be considered (Yin et al.,  
568 2021).—The activation of the signalling network mTOR has been associated with organic and inorganic  
569 contaminants-induced apoptosis (Chen et al., 2008; McCuaig et al., 2020). Moreover, the ADP/ATP  
570 translocase is suggested to play a significant role in the process of mitochondrial permeabilization as it  
571 can switch its function from ADP/ATP exchange through inner mitochondrial membrane to pore-  
572 formation during apoptosis (Kumarswamy & Chandna, 2009). Therefore, these two proteins could be  
573 excellent candidates biomarker for trace element effects in liver in red muscle.



574

575 **Metabolism and immune system up-regulation in liver**

576 Trace element contamination (mixtures 1 and 3) appeared to specifically affect the metabolism and  
577 transport of lipids in the liver, as reflected by the overexpression of two apolipoproteins (hubproteins).  
578 Lipids are an energy source and an essential component of cell membranes (phospholipids and  
579 cholesterol). Besides, they also play a significant role as messengers in signal transduction pathways and  
580 molecular recognition processes (Van Meer et al., 2008). Any changes in lipid metabolism would signal  
581 impairment of these pathways. It has been reported that constant energy demand leads to mobilization  
582 of triglycerides as they serve as lipid storage (Van Meer et al., 2008; Santos and Schulze 2012). The  
583 upregulation of triglyceride metabolic process and transport underlined in this study could be an  
584 evidence of their mobilization and use in repair or development of membranes damaged, for instance  
585 under increasing oxidative stress (Van Meer et al., 2008; Santos and Schulze 2012). ~~(Santos and Schulze~~  
586 ~~2012)~~. Their mobilization and transport may also be linked to low food intake or absorption due to gut  
587 damage or improper synthesis in the liver under trace element stress. In the absence of further research  
588 to shed light on these regulation patterns, we propose here two promising biomarkers that may indicate  
589 a dysregulation in lipid transport and metabolism in response to contamination: apolipoprotein B-100  
590 and apolipoprotein A-IV (see Table 2) that were found upregulated in our study but also in seahorses and  
591 atlantic cod in response to heavy metal and organic contaminant stress respectively (Bohne-Kjersem et  
592 al., 2009; Liu et al., 2022). These proteins are important regulators of triglyceride and cholesterol  
593 metabolism (Sacks, 2006). By studying these potential biomarkers, we can gain valuable insights into the  
594 effects of metal contamination on lipid-related processes.

595 The sardine liver proteome also presented a clear up-regulation in multiple pathways involved in  
596 immune processes. Regoli & Giuliani (2014) and Wang & Gallagher (2013) highlighted that such an up-  
597 regulation could be related to trace element accumulation in the liver and lead to increasing oxidative  
598 stress. The fish immune system is known to be sensitive to environmental contamination (Si et al., 2019)  
599 and altering immune homeostasis in fish could significantly constrain their survival and development.  
600 Sustaining high levels of immune functions requires energy, which would be necessarily redirected from  
601 other main functions, such as growth, reproduction or maintenance (energy trade-off, ; Moret &  
602 Schmid-Hempel, 2000).

603 In our experiment we did not find any correlation between body condition and contamination  
604 mixtures. This is consistent with some other studies that investigated the relationship between metal  
605 levels in the environment or fish tissues and body condition (Frag et al., 1998; Dethloff et al., 2001;  
606 Lohner et al., 2001). The measurement of body mass may not sufficiently illustrate the costs of metal  
607 exposure, since individuals can balance their resource budget and adjust their body condition over a  
608 longer period (Daan et al., 1996, Beauvieux et al., 2022). The absence of relationship could also suggest  
609 that body condition, although a great marker of nutritional stress (Brosset et al., 2015), only declines  
610 drastically when a high threshold of physiological stress is reached. Therefore, monitoring physiological  
611 processes that are more sensitive and reflect progressive changes might allow to detect early warnings of  
612 environmental challenges. Nonetheless, sardines from the Mediterranean Sea have shown a drastic  
613 decline in body condition, size and life expectancy in the past two decades (Saraux et al., 2019). The  
614 major driver proposed is the shift of sardine diet towards smaller planktonic prey observed in the Gulf of  
615 Lions due to multi-factorial environmental changes (Feuillolley et al 2020, Brosset et al., 2016), leading to  
616 lower foraging efficiency and a reallocation trade-off toward reproduction instead of survival (Beauvieux  
617 et al., 2022; Queiros et al., 2019, 2024). Consequently, individuals at the end of the reproduction period  
618 may rely on low energetic reserves to survive the end of the winter period. Adding any additional  
619 energetic or immune burden, as those highlighted in response to contaminants in this study, might  
620 emphasize their reduced chance of survival (Queiros et al., 2021).

621

622

### Acknowledgements

623 We are grateful to the technical and scientific crews of L'Europe for their work during PELMED survey.  
624 Furthermore, we thank Sophie Prud'homme, Roberta Bettinetti and an anonymous reviewer for their  
625 valuable inputs and comments on this manuscript.

626

### Data, scripts, code, and supplementary information availability

627 The mass spectrometry proteomics data have been deposited to the ProteomeXchange Consortium  
628 via the PRIDE (Perez-Riverol et al., 2019) partner repository with the dataset identifiers PXD037276 (liver)  
629 and PXD037313 (red muscle).

630 Scripts, figures 5 and 7 and other datasets are available online:  
631 <https://doi.org/10.5281/zenodo.10683281>

632

### Conflict of interest disclosure

633 The authors declare that they comply with the PCI rule of having no financial conflicts of interest in  
634 relation to the content of the article.

635

### Funding

636 This work is part of the project ICIPOP granted by the “Agence Francaise de Developpement” (AFD).  
637 A. B. has a PhD grant from University of Montpellier – GAIA doctoral school.  
638

639

### References

640 Alekseenko, E., Thouvenin, B., Tronczyński, J., Carlotti, F., Garreau, P., Tixier, C., & Baklouti, M. (2018).  
641 Modeling of PCB trophic transfer in the Gulf of Lions; 3D coupled model application. *Marine Pollution*  
642 *Bulletin*, 128, 140–155. <https://doi.org/10.1016/j.marpolbul.2018.01.008>

643 Apraiz, I., Mi, J., & Cristobal, S. (2006). Identification of proteomic signatures of exposure to marine pollutants  
644 in mussels (*Mytilus edulis*). *Molecular and Cellular Proteomics*, 5(7), 1274–1285.  
645 <https://doi.org/10.1074/mcp.M500333-MCP200>

646 Asaduzzaman, K., Khandaker, M. U., Binti Baharudin, N. A., Amin, Y. B. M., Farook, M. S., Bradley, D. A., &  
647 Mahmoud, O. (2017). Heavy metals in human teeth dentine: A bio-indicator of metals exposure and  
648 environmental pollution. *Chemosphere*, 176, 221–230.  
649 <https://doi.org/10.1016/j.chemosphere.2017.02.114>

650 Asker, N., Kristiansson, E., Albertsson, E., Larsson, D. G. J., & Förlin, L. (2013). Hepatic transcriptome profiling  
651 indicates differential mRNA expression of apoptosis and immune related genes in eelpout (*Zoarces*  
652 *viviparus*) caught at Göteborg harbor, Sweden. *Aquatic Toxicology*, 130–131, 58–67.  
653 <https://doi.org/10.1016/j.aquatox.2012.12.017>

654 Aslam, S., & Yousafzai, A. M. (2017). Chromium toxicity in fish: A review article. ~ 1483 ~ *Journal of Entomology*  
655 *and Zoology Studies*, 5(3), 1483–1488.

656 Authman, M. M. N. (2011). Environmental and experimental studies of aluminium toxicity on the liver of  
657 *Oreochromis niloticus* (Linnaeus, 1757) fish. *Life Science Journal*, 8(4), 764–776.

658 Baker, E., Sevaldsen, P., & Kurvits, T. (2013). State and pressures of the marine and coastal Mediterranean  
659 environment. In *European Environment Agency* (Issue 5).

660 Bawuro, A. A., Voegborlo, R. B., & Adimado, A. A. (2018). Bioaccumulation of Heavy Metals in Some Tissues of  
661 Fish in Lake Geriyo, Adamawa State, Nigeria. *Journal of Environmental and Public Health*, 2018.  
662 <https://doi.org/10.1155/2018/1854892>

663 Beauvieux, A., Fromentin, J.-M., Romero, D., Couffin, N., Brown, A., Metral, L., Bourjea, J., Bertile, F., & Schull,

- 664 Q. (2024). Molecular fingerprint of gilthead seabream physiology in response to pollutant mixtures in the  
665 wild. *Environmental Pollution*, 340, 122789. <https://doi.org/10.1016/j.envpol.2023.122789>
- 666 Beauvieux, A., Queiros, Q., Metral, L., Dutto, G., Gasset, E., Criscuolo, F., Fromentin, J. M., Saraux, C., & Schull,  
667 Q. (2022). Energy allocation trade-offs between life-history traits in the Mediterranean sardine: an  
668 ecophysiological approach. *Marine Ecology Progress Series*, 701(Stearns 1989), 99–118.  
669 <https://doi.org/10.3354/meps14183>
- 670 Benninghoff, A. D. (2007). Toxicoproteomics - The next step in the evolution of environmental biomarkers?  
671 *Toxicological Sciences*, 95(1), 1–4. <https://doi.org/10.1093/toxsci/kfl157>
- 672 Bervoets, L., & Blust, R. (2003). Metal concentrations in water, sediment and gudgeon (*Gobio gobio*) from a  
673 pollution gradient: Relationship with fish condition factor. *Environmental Pollution*, 126(1), 9–19.  
674 [https://doi.org/10.1016/S0269-7491\(03\)00173-8](https://doi.org/10.1016/S0269-7491(03)00173-8)
- 675 Bervoets, L., Knaepkens, G., Eens, M., & Blust, R. (2005). Fish community responses to metal pollution.  
676 *Environmental Pollution*, 138(2), 338–349. <https://doi.org/10.1016/j.envpol.2005.03.005>
- 677 Bindea, G., Mlecnik, B., Hackl, H., Charoentong, P., Tosolini, M., Kirilovsky, A., Fridman, W.-H., Pagès, F.,  
678 Trajanoski, Z., & Galon, J. (2009). ClueGO: a Cytoscape plug-in to decipher functionally grouped gene  
679 ontology and pathway annotation networks. *Bioinformatics*, 25(8), 1091–1093.  
680 <https://doi.org/10.1093/bioinformatics/btp101>
- 681 Blewett, T. A., & Leonard, E. M. (2017). Mechanisms of nickel toxicity to fish and invertebrates in marine and  
682 estuarine waters. *Environmental Pollution*, 223, 311–322. <https://doi.org/10.1016/j.envpol.2017.01.028>
- 683 Bodiguel, X., Loizeau, V., Le Guellec, A. M., Roupsard, F., Philippon, X., & Mellon-Duval, C. (2009). Influence of  
684 sex, maturity and reproduction on PCB and p,p'DDE concentrations and repartitions in the European  
685 hake (*Merluccius merluccius*, L.) from the Gulf of Lions (N.W. Mediterranean). *Science of the Total  
686 Environment*, 408(2), 304–311. <https://doi.org/10.1016/j.scitotenv.2009.10.004>
- 687 Bohne-Kjersem, A., Skadsheim, A., Goksøyr, A., & Grøsvik, B. E. (2009). Candidate biomarker discovery in  
688 plasma of juvenile cod (*Gadus morhua*) exposed to crude North Sea oil, alkyl phenols and polycyclic  
689 aromatic hydrocarbons (PAHs). *Marine Environmental Research*, 68(5), 268–277.  
690 <https://doi.org/10.1016/j.marenvres.2009.06.016>
- 691 Bouchoucha, M. (2021). *SUCHI Med 2021*. <https://doi.org/https://doi.org/10.17600/18001619>
- 692 Bourdeix, J., & Hattab, T. (1985). *PELMED - PELAGIQUES MEDITERRANÉE*. <https://doi.org/10.18142/19>
- 693 Boyle, E. A., Chapnick, S. D., Bai, X. X., & Spivack, A. (1985). Trace metal enrichments in the Mediterranean Sea.  
694 *Earth and Planetary Science Letters*, 74(4), 405–419. [https://doi.org/10.1016/S0012-821X\(85\)80011-X](https://doi.org/10.1016/S0012-821X(85)80011-X)
- 695 Braasch, I., Gehrke, A. R., Smith, J. J., Kawasaki, K., Manousaki, T., Pasquier, J., Amores, A., Desvignes, T.,  
696 Batzel, P., Catchen, J., Berlin, A. M., Campbell, M. S., Barrell, D., Martin, K. J., Mulley, J. F., Ravi, V., Lee, A.  
697 P., Nakamura, T., Chalopin, D., ... Postlethwait, J. H. (2016). The spotted gar genome illuminates  
698 vertebrate evolution and facilitates human-teleost comparisons. *Nature Genetics*, 48(4), 427–437.  
699 <https://doi.org/10.1038/ng.3526>
- 700 Broche, P., Devenon, J. L., Forget, P., De Maistre, J. C., Naudin, J. J., & Cauwet, G. (1998). Experimental study of  
701 the Rhone plume. Part I: Physics and dynamics. *Oceanologica Acta*, 21(6), 725–738.  
702 [https://doi.org/10.1016/S0399-1784\(99\)80002-4](https://doi.org/10.1016/S0399-1784(99)80002-4)
- 703 Brosset, P., Fromentin, J. M., Ménard, F., Pernet, F., Bourdeix, J. H., Bigot, J. L., Van Beveren, E., Pérez Roda, M.  
704 A., Choy, S., & Saraux, C. (2015). Measurement and analysis of small pelagic fish condition: A suitable  
705 method for rapid evaluation in the field. *Journal of Experimental Marine Biology and Ecology*, 462, 90–

- 706           97. <https://doi.org/10.1016/j.jembe.2014.10.016>
- 707   Brosset, P., Fromentin, J. M., Van Beveren, E., Lloret, J., Marques, V., Basilone, G., Bonanno, A., Carpi, P.,  
708       Donato, F., Čikeš Keč, V., De Felice, A., Ferreri, R., Gašparević, D., Giráldez, A., Gücü, A., Iglesias, M.,  
709       Leonori, I., Palomera, I., Somarakis, S., ... Saraux, C. (2017). Spatio-temporal patterns and environmental  
710       controls of small pelagic fish body condition from contrasted Mediterranean areas. *Progress in*  
711       *Oceanography*, 151(February), 149–162. <https://doi.org/10.1016/j.pocean.2016.12.002>
- 712   Brosset, P., Le Bourg, B., Costalago, D., Bănar, D., Van Beveren, E., Bourdeix, J. H., Fromentin, J. M., Ménard,  
713       F., & Saraux, C. (2016). Linking small pelagic dietary shifts with ecosystem changes in the Gulf of Lions.  
714       *Marine Ecology Progress Series*, 554, 157–171. <https://doi.org/10.3354/meps11796>
- 715   Brosset, P., Ménard, F., Fromentin, J. M., Bonhommeau, S., Ulses, C., Bourdeix, J. H., Bigot, J. L., Van Beveren,  
716       E., Roos, D., & Saraux, C. (2015). Influence of environmental variability and age on the body condition of  
717       small pelagic fish in the Gulf of Lions. *Marine Ecology Progress Series*, 529, 219–231.  
718       <https://doi.org/10.3354/meps11275>
- 719   Bucchia, M., Camacho, M., Santos, M. R. D., Boada, L. D., Roncada, P., Mateo, R., Ortiz-Santaliestra, M. E.,  
720       Rodríguez-Estival, J., Zumbado, M., Orós, J., Henríquez-Hernández, L. A., García-Álvarez, N., & Luzardo, O.  
721       P. (2015). Plasma levels of pollutants are much higher in loggerhead turtle populations from the Adriatic  
722       Sea than in those from open waters (Eastern Atlantic Ocean). *Science of the Total Environment*, 523,  
723       161–169. <https://doi.org/10.1016/j.scitotenv.2015.03.047>
- 724   Carapito, C., Burel, A., Guterl, P., Walter, A., Varrier, F., Bertile, F., & Van Dorsselaer, A. (2014). MSDA, a  
725       proteomics software suite for in-depth Mass Spectrometry Data Analysis using grid computing.  
726       *Proteomics*, 14(9), 1014–1019. <https://doi.org/10.1002/pmic.201300415>
- 727   Celander, M. C. (2011). Cocktail effects on biomarker responses in fish. *Aquatic Toxicology*, 105(3–4), 72–77.  
728       <https://doi.org/10.1016/j.aquatox.2011.06.002>
- 729   Chen, L., Liu, L., Luo, Y., & Huang, S. (2008). MAPK and mTOR pathways are involved in cadmium-induced  
730       neuronal apoptosis. *Journal of Neurochemistry*, 105(1), 251–261. [https://doi.org/10.1111/j.1471-](https://doi.org/10.1111/j.1471-4159.2007.05133.x)  
731       [4159.2007.05133.x](https://doi.org/10.1111/j.1471-4159.2007.05133.x)
- 732   Chouvelon, T., Cresson, P., Bouchouca, M., Brach-Papa, C., Bustamante, P., Crochet, S., Marco-Miralles, F.,  
733       Thomas, B., & Knoery, J. (2018). Oligotrophy as a major driver of mercury bioaccumulation in medium-to  
734       high-trophic level consumers: A marine ecosystem-comparative study. *Environmental Pollution*, 233,  
735       844–854. <https://doi.org/10.1016/j.envpol.2017.11.015>
- 736   Chouvelon, T., Strady, E., Harmelin-Vivien, M., Radakovitch, O., Brach-Papa, C., Crochet, S., Knoery, J., Rozuel,  
737       E., Thomas, B., Tronczynski, J., & Chiffolleau, J.-F. (2019). Patterns of trace metal bioaccumulation and  
738       trophic transfer in a phytoplankton-zooplankton-small pelagic fish marine food web. *Marine Pollution*  
739       *Bulletin*, 146, 1013–1030. <https://doi.org/10.1016/j.marpolbul.2019.07.047>
- 740   Cossa, D., & Coquery, M. (2005). *The Mediterranean Mercury Anomaly, a Geochemical or a Biological Issue*  
741       (Vol. 5, Issue June, pp. 177–208). <https://doi.org/10.1007/b107147>
- 742   Cossa, D., Durrieu de Madron, X., Schäfer, J., Lanceleur, L., Guédron, S., Buscaïl, R., Thomas, B., Castelle, S., &  
743       Naudin, J. J. (2017). The open sea as the main source of methylmercury in the water column of the Gulf  
744       of Lions (Northwestern Mediterranean margin). *Geochimica et Cosmochimica Acta*, 199, 222–237.  
745       <https://doi.org/10.1016/j.gca.2016.11.037>
- 746   Danovaro, R. (2003). Pollution threats in the Mediterranean Sea : An overview. *Chemistry and Ecology*, 19(1),  
747       15–32. <https://doi.org/10.1080/0275754031000081467>
- 748   Denslow, N. D., Knoeb, I., & Larkin, P. (2005). Chapter 3 Approaches in proteomics and genomics for eco-

- 749 toxicology. *Biochemistry and Molecular Biology of Fishes*, 6(C), 85–116. [https://doi.org/10.1016/S1873-](https://doi.org/10.1016/S1873-0140(05)80006-2)  
750 [0140\(05\)80006-2](https://doi.org/10.1016/S1873-0140(05)80006-2)
- 751 Dethloff, G. M., Bailey, H. C., & Maier, K. J. (2001). Effects of dissolved copper on select hematological,  
752 biochemical, and immunological parameters of wild rainbow trout (*Oncorhynchus mykiss*). *Archives of*  
753 *Environmental Contamination and Toxicology*, 40(3), 371–380. <https://doi.org/10.1007/s002440010185>
- 754 Dixon, G. B., Davies, S. W., Aglyamova, G. V., Meyer, E., Bay, L. K., & Matz, M. V. (2015). Genomic determinants  
755 of coral heat tolerance across latitudes. *Science*, 348(6242), 1460–1462.  
756 <https://doi.org/10.1126/science.1261224>
- 757 Downs, C. A., Richmond, R. H., Mendiola, W. J., Rougée, L., & Ostrander, G. K. (2006). Cellular physiological  
758 effects of the MV Kyowa Violet fuel-oil spill on the hard coral, *Porites lobata*. *Environmental Toxicology*  
759 *and Chemistry*, 25(12), 3171–3180. <https://doi.org/10.1897/05-509R1.1>
- 760 Durrieu de Madron, X., Guieu, C., Sempéré, R., Conan, P., Cossa, D., D’Ortenzio, F., Estournel, C., Gazeau, F.,  
761 Rabouille, C., Stemmann, L., Bonnet, S., Diaz, F., Koubbi, P., Radakovitch, O., Babin, M., Baklouti, M.,  
762 Bancon-Montigny, C., Belviso, S., Bensoussan, N., ... Verney, R. (2011). Marine ecosystems’ responses to  
763 climatic and anthropogenic forcings in the Mediterranean. *Progress in Oceanography*, 91(2), 97–166.  
764 <https://doi.org/10.1016/j.pocean.2011.02.003>
- 765 Dydak, U., Jiang, Y. M., Long, L. L., Zhu, H., Chen, J., Li, W. M., Edden, R. A. E., Hu, S., Fu, X., Long, Z., Mo, X. A.,  
766 Meier, D., Harezlak, J., Aschner, M., Murdoch, J. B., & Zheng, W. (2011). In vivo measurement of brain  
767 GABA concentrations by magnetic resonance spectroscopy in smelters occupationally exposed to  
768 manganese. *Environmental Health Perspectives*, 119(2), 219–224. <https://doi.org/10.1289/ehp.1002192>
- 769 Epel, E. S., Blackburn, E. H., Lin, J., Dhabhar, F. S., Adler, N. E., Morrow, J. D., & Cawthon, R. M. (2004).  
770 Accelerated telomere shortening in response to life stress. *Proceedings of the National Academy of*  
771 *Sciences of the United States of America*, 101(49), 17312–17315.  
772 <https://doi.org/10.1073/pnas.0407162101>
- 773 Exley, C., Chappell, J. S., & Birchall, J. D. (1991). A mechanism for acute aluminium toxicity in fish. *Journal of*  
774 *Theoretical Biology*, 151(3), 417–428. [https://doi.org/10.1016/S0022-5193\(05\)80389-3](https://doi.org/10.1016/S0022-5193(05)80389-3)
- 775 Farag, A. M., Woodward, D. F., Goldstein, J. N., Brumbaugh, W., & Meyer, J. S. (1998). Concentrations of  
776 metals associated with mining waste in sediments, biofilm, benthic macroinvertebrates, and fish from  
777 the Coeur d’Alene River Basin, Idaho. *Archives of Environmental Contamination and Toxicology*, 34(2),  
778 119–127. <https://doi.org/10.1007/s002449900295>
- 779 Feuilletoy, G., Fromentin, J. M., Stemmann, L., Demarcq, H., Estournel, C., & Saraux, C. (2020). Concomitant  
780 changes in the environment and small pelagic fish community of the Gulf of Lions. *Progress in*  
781 *Oceanography*, 186(June), 102375. <https://doi.org/10.1016/j.pocean.2020.102375>
- 782 Folch, J., Lees, M., & Stanley, G. H. S. (1957). A simple method for the isolation and purification of total lipides  
783 from animal tissues. *Journal of Biological Chemistry*, 226(1), 497–509. [https://doi.org/10.1016/S0021-](https://doi.org/10.1016/S0021-9258(18)64849-5)  
784 [9258\(18\)64849-5](https://doi.org/10.1016/S0021-9258(18)64849-5)
- 785 Friberg, L., Nordberg, G. F., & Vouk, V. B. (1979). *Handbook of the toxicology of metals*. Elsevier/North-Holland  
786 Biomedical Press.
- 787 Gabrielides, G. P. (1995). Pollution of the Mediterranean Sea. *Water Science and Technology*, 32(9–10), 1–10.  
788 [https://doi.org/10.1016/0273-1223\(96\)00070-4](https://doi.org/10.1016/0273-1223(96)00070-4)
- 789 Genchi, G., Carocci, A., Lauria, G., Sinicropi, M. S., & Catalano, A. (2021). Thallium Use, Toxicity, and  
790 Detoxification Therapy: An Overview. *Applied Sciences*, 11(18), 8322.  
791 <https://doi.org/10.3390/app11188322>

- 792 Guérin, T., Chekri, R., Vastel, C., Sirot, V., Volatier, J. L., Leblanc, J. C., & Noël, L. (2011). Determination of 20  
793 trace elements in fish and other seafood from the French market. *Food Chemistry*, 127(3), 934–942.  
794 <https://doi.org/10.1016/j.foodchem.2011.01.061>
- 795 Guerra-García, J. M., Calero-Cano, S., Donázar-Aramendía, Í., Giráldez, I., Morales, E., Arechavala-Lopez, P., &  
796 Cervera-Currado, J. L. (2023). Assessment of elemental composition in commercial fish of the Bay of  
797 Cádiz, Southern Iberian Peninsula. *Marine Pollution Bulletin*, 187(November 2022).  
798 <https://doi.org/10.1016/j.marpolbul.2022.114504>
- 799 Guo, Z., Zhang, W., Du, S., Green, I., Tan, Q., & Zhang, L. (2016). Developmental patterns of copper  
800 bioaccumulation in a marine fish model *Oryzias melastigma*. *Aquatic Toxicology*, 170, 216–222.  
801 <https://doi.org/10.1016/j.aquatox.2015.11.026>
- 802 Halliwell, B., & Gutteridge, J. M. C. (2015). *Free Radicals in Biology and Medicine*. Oxford University Press.  
803 <https://doi.org/10.1093/acprof:oso/9780198717478.001.0001>
- 804 Harmelin-Vivien, M., Cossa, D., Crochet, S., Bănar, D., Letourneur, Y., & Mellon-Duval, C. (2009). Difference of  
805 mercury bioaccumulation in red mullets from the north-western Mediterranean and Black seas. *Marine*  
806 *Pollution Bulletin*, 58(5), 679–685. <https://doi.org/10.1016/j.marpolbul.2009.01.004>
- 807 Heys, K. A., Shore, R. F., Pereira, M. G., Jones, K. C., & Martin, F. L. (2016). Risk assessment of environmental  
808 mixture effects. *RSC Advances*, 6(53), 47844–47857. <https://doi.org/10.1039/c6ra05406d>
- 809 Hollis, L., McGeer, J. C., McDonald, D. G., & Wood, C. M. (1999). Cadmium accumulation, gill Cd binding,  
810 acclimation, and physiological effects during long term sublethal Cd exposure in rainbow trout. *Aquatic*  
811 *Toxicology*, 46(2), 101–119. [https://doi.org/10.1016/S0166-445X\(98\)00118-0](https://doi.org/10.1016/S0166-445X(98)00118-0)
- 812 Isani, G., Andreani, G., Cocchioni, F., Fedeli, D., Carpené, E., & Falcioni, G. (2009). Cadmium accumulation and  
813 biochemical responses in *Sparus aurata* following sub-lethal Cd exposure. *Ecotoxicology and*  
814 *Environmental Safety*, 72(1), 224–230. <https://doi.org/10.1016/j.ecoenv.2008.04.015>
- 815 Jaishankar, M., Tseten, T., Anbalagan, N., Mathew, B. B., & Beeregowda, K. N. (2014). Toxicity , mechanism and  
816 health effects of some heavy metals. *Interdisciplinary Toxicology*, 7(2), 60–72.  
817 <https://doi.org/10.2478/intox-2014-0009>
- 818 Javed, M., Ahmad, M. I., Usmani, N., & Ahmad, M. (2017). Multiple biomarker responses (serum biochemistry,  
819 oxidative stress, genotoxicity and histopathology) in *Channa punctatus* exposed to heavy metal loaded  
820 waste water. *Scientific Reports*, 7(1), 1675. <https://doi.org/10.1038/s41598-017-01749-6>
- 821 Joiris, C. R., Holsbeek, L., & Moatemri, N. L. (1999). Total and methylmercury in sardines *Sardinella aurita* and  
822 *Sardina pilchardus* from Tunisia. *Marine Pollution Bulletin*, 38(3), 188–192.  
823 [https://doi.org/10.1016/S0025-326X\(98\)00171-4](https://doi.org/10.1016/S0025-326X(98)00171-4)
- 824 Kardon, J. R., & Vale, R. D. (2009). Regulators of the cytoplasmic dynein motor. *Nature Reviews Molecular Cell*  
825 *Biology*, 10(12), 854–865. <https://doi.org/10.1038/nrm2804>
- 826 Karim, M., Puiseux-Dao, S., & Edery, M. (2011). Toxins and stress in fish: Proteomic analyses and response  
827 network. *Toxicol*, 57(7–8), 959–969. <https://doi.org/10.1016/j.toxicol.2011.03.018>
- 828 Kaushal, S. S., Gold, A. J., Bernal, S., Johnson, T. A. N., Addy, K., Burgin, A., Burns, D. A., Coble, A. A., Hood, E.,  
829 Lu, Y. H., Mayer, P., Minor, E. C., Schroth, A. W., Vidon, P., Wilson, H., Xenopoulos, M. A., Doody, T.,  
830 Galella, J. G., Goodling, P., ... Belt, K. T. (2018). Watershed ‘chemical cocktails’: forming novel elemental  
831 combinations in Anthropocene fresh waters. *Biogeochemistry*, 141(3), 281–305.  
832 <https://doi.org/10.1007/s10533-018-0502-6>
- 833 Koivula, M. J., & Eeva, T. (2010). Metal-related oxidative stress in birds. *Environmental Pollution*, 158(7), 2359–

- 834 2370. <https://doi.org/10.1016/j.envpol.2010.03.013>
- 835 Kumari, B., Kumar, V., Sinha, A. K., Ahsan, J., Ghosh, A. K., Wang, H., & DeBoeck, G. (2017). Toxicology of  
836 arsenic in fish and aquatic systems. *Environmental Chemistry Letters*, 15(1), 43–64.  
837 <https://doi.org/10.1007/s10311-016-0588-9>
- 838 Kumarswamy, R., & Chandna, S. (2009). Putative partners in Bax mediated cytochrome-c release: ANT, CypD,  
839 VDAC or none of them? *Mitochondrion*, 9(1), 1–8. <https://doi.org/10.1016/j.mito.2008.10.003>
- 840 Langfelder, P., & Horvath, S. (2008). WGCNA: An R package for weighted correlation network analysis. *BMC*  
841 *Bioinformatics*, 9. <https://doi.org/10.1186/1471-2105-9-559>
- 842 Le Bourg, B., Bănar, D., Sarau, C., Nowaczyk, A., Le Luherne, E., Jadaud, A., Bigot, J. L., & Richard, P. (2015).  
843 Trophic niche overlap of sprat and commercial small pelagic teleosts in the Gulf of Lions (NW  
844 Mediterranean Sea). *Journal of Sea Research*, 103, 138–146.  
845 <https://doi.org/10.1016/j.seares.2015.06.011>
- 846 Leaver, M. J., Diab, A., Boukouvala, E., Williams, T. D., Chipman, J. K., Moffat, C. F., Robinson, C. D., & George,  
847 S. G. (2010). Hepatic gene expression in flounder chronically exposed to multiply polluted estuarine  
848 sediment: Absence of classical exposure “biomarker” signals and induction of inflammatory, innate  
849 immune and apoptotic pathways. *Aquatic Toxicology*, 96(3), 234–245.  
850 <https://doi.org/10.1016/j.aquatox.2009.10.025>
- 851 Li, Y., & Wang, W. X. (2021). Integrated transcriptomics and proteomics revealed the distinct toxicological  
852 effects of multi-metal contamination on oysters. *Environmental Pollution*, 284(June), 117533.  
853 <https://doi.org/10.1016/j.envpol.2021.117533>
- 854 Liu, Y., Shang, D., Yang, Y., Cui, P., & Sun, J. (2022). Transcriptomic Analysis Provides Insights into Microplastic  
855 and Heavy Metal Challenges in the Line Seahorse (*Hippocampus erectus*). *Fishes*, 7(6), 338.  
856 <https://doi.org/10.3390/fishes7060338>
- 857 Lloret, J., Shulman, G., & Love, R. M. (2013). Condition and Health Indicators of Exploited Marine Fishes. In  
858 *Condition and Health Indicators of Exploited Marine Fishes*. John Wiley & Sons.  
859 <https://doi.org/10.1002/9781118752777>
- 860 Lohner, T. W., Reash, R. J., Willet, V. E., & Rose, L. A. (2001). Assessment of tolerant sunfish populations  
861 (*Lepomis* sp.) inhabiting selenium-laden coal ash effluents: 1. Hematological and population level  
862 assessment. *Ecotoxicology and Environmental Safety*, 50(3), 203–216.  
863 <https://doi.org/10.1006/eesa.2001.2097>
- 864 López-Pedrouso, M., Varela, Z., Franco, D., Fernández, J. A., & Aboal, J. R. (2020). Can proteomics contribute to  
865 biomonitoring of aquatic pollution? A critical review. In *Environmental Pollution* (Vol. 267, p. 115473).  
866 Elsevier Ltd. <https://doi.org/10.1016/j.envpol.2020.115473>
- 867 Lozano-Bilbao, E., Díaz, Y., Lozano, G., Jurado-Ruzafa, A., Hardisson, A., Rubio, C., Jiménez, S., González-Weller,  
868 D., & Gutiérrez, Á. J. (2019). Metal Content in Small Pelagic Fish in the North-West Africa. *Thalassas*,  
869 35(2), 643–653. <https://doi.org/10.1007/s41208-019-00141-7>
- 870 McCuaig, L. M., Martyniuk, C. J., & Marlatt, V. L. (2020). Morphometric and proteomic responses of early-life  
871 stage rainbow trout (*Oncorhynchus mykiss*) to the aquatic herbicide diquat dibromide. *Aquatic*  
872 *Toxicology*, 222, 105446. <https://doi.org/10.1016/j.aquatox.2020.105446>
- 873 Mela, M., Randi, M. A. F., Ventura, D. F., Carvalho, C. E. V., Pelletier, E., & Oliveira Ribeiro, C. A. (2007). Effects  
874 of dietary methylmercury on liver and kidney histology in the neotropical fish *Hoplias malabaricus*.  
875 *Ecotoxicology and Environmental Safety*, 68(3), 426–435. <https://doi.org/10.1016/j.ecoenv.2006.11.013>

- 876 Mitra, A., Shevde, L. A., & Samant, R. S. (2009). Multi-faceted role of HSP40 in cancer. *Clinical and Experimental*  
877 *Metastasis*, 26(6), 559–567. <https://doi.org/10.1007/s10585-009-9255-x>
- 878 Mollan, T. L., Khandros, E., Weiss, M. J., & Olson, J. S. (2012). Kinetics of  $\alpha$ -globin binding to  $\alpha$ -Hemoglobin  
879 Stabilizing Protein (AHSP) indicate preferential stabilization of hemichrome folding intermediate. *Journal*  
880 *of Biological Chemistry*, 287(14), 11338–11350. <https://doi.org/10.1074/jbc.M111.313247>
- 881 Morcillo, P., Esteban, M., & Cuesta, A. (2016). Heavy metals produce toxicity, oxidative stress and apoptosis in  
882 the marine teleost fish SAF-1 cell line. *Chemosphere*, 144, 225–233.  
883 <https://doi.org/10.1016/j.chemosphere.2015.08.020>
- 884 Moreira, C. M., Oliveira, E. M., Bonan, C. D., Sarkis, J. J. F., & Vassallo, D. V. (2003). Effects of mercury on  
885 myosin ATPase in the ventricular myocardium of the rat. *Comparative Biochemistry and Physiology - C*  
886 *Toxicology and Pharmacology*, 135(3), 269–275. [https://doi.org/10.1016/S1532-0456\(03\)00110-8](https://doi.org/10.1016/S1532-0456(03)00110-8)
- 887 Moret, Y., & Schmid-Hempel, P. (2000). Survival for immunity: The price of immune system activation for  
888 bumblebee workers. *Science*, 290(5494), 1166–1168. <https://doi.org/10.1126/science.290.5494.1166>
- 889 Parrish, C. C. (1988). Dissolved and particulate marine lipid classes: a review. *Marine Chemistry*, 23(1–2), 17–  
890 40. [https://doi.org/10.1016/0304-4203\(88\)90020-5](https://doi.org/10.1016/0304-4203(88)90020-5)
- 891 Paschal, B. M., Shpetner, H. S., & Vallee, R. B. (1987). MAP 1C is a microtubule-activated ATPase which  
892 translocates microtubules in vitro and has dynein-like properties. *Journal of Cell Biology*, 105(3), 1273–  
893 1282. <https://doi.org/10.1083/jcb.105.3.1273>
- 894 Pedrotti, M. L., Petit, S., Elineau, A., Bruzaud, S., Crebassa, J. C., Dumontet, B., Martí, E., Gorsky, G., & Cózar, A.  
895 (2016). Changes in the floating plastic pollution of the mediterranean sea in relation to the distance to  
896 land. *PLoS ONE*, 11(8), 1–14. <https://doi.org/10.1371/journal.pone.0161581>
- 897 Pereira, S., Pinto, A. L., Cortes, R., Fontainhas-Fernandes, A., Coimbra, A. M., & Monteiro, S. M. (2013). Gill  
898 histopathological and oxidative stress evaluation in native fish captured in Portuguese northwestern  
899 rivers. *Ecotoxicology and Environmental Safety*, 90, 157–166.  
900 <https://doi.org/10.1016/j.ecoenv.2012.12.023>
- 901 Perez-Riverol, Y., Csordas, A., Bai, J., Bernal-Llinares, M., Hewapathirana, S., Kundu, D. J., Inuganti, A., Griss, J.,  
902 Mayer, G., Eisenacher, M., Pérez, E., Uszkoreit, J., Pfeuffer, J., Sachsenberg, T., Yilmaz, Ş., Tiwary, S., Cox,  
903 J., Audain, E., Walzer, M., ... Vizcaíno, J. A. (2019). The PRIDE database and related tools and resources in  
904 2019: Improving support for quantification data. *Nucleic Acids Research*, 47(D1), D442–D450.  
905 <https://doi.org/10.1093/nar/gky1106>
- 906 Plum, L. M., Rink, L., & Hajo, H. (2010). The essential toxin: Impact of zinc on human health. *International*  
907 *Journal of Environmental Research and Public Health*, 7(4), 1342–1365.  
908 <https://doi.org/10.3390/ijerph7041342>
- 909 Queiros, Q., Fromentin, J. M., Gasset, E., Dutto, G., Huiban, C., Metral, L., Leclerc, L., Schull, Q., McKenzie, D. J.,  
910 & Sarau, C. (2019). Food in the sea: Size also matters for pelagic fish. *Frontiers in Marine Science*, 6(JUL),  
911 385. <https://doi.org/10.3389/fmars.2019.00385>
- 912 Queiros, Q., Mckenzie, D. J., Dutto, G., Killen, S., Sarau, C., & Schull, Q. (2024). Fish shrinking , energy balance  
913 and climate change. *Science of the Total Environment*, 906, 167310.  
914 <https://doi.org/10.1016/j.scitotenv.2023.167310>
- 915 Radakovitch, O., Roussiez, V., Ollivier, P., Ludwig, W., Grenz, C., & Probst, J. L. (2008). Input of particulate  
916 heavy metals from rivers and associated sedimentary deposits on the Gulf of Lion continental shelf.  
917 *Estuarine, Coastal and Shelf Science*, 77(2), 285–295. <https://doi.org/10.1016/j.ecss.2007.09.028>



- 918 Regoli, F., & Giuliani, M. E. (2014). Oxidative pathways of chemical toxicity and oxidative stress biomarkers in  
919 marine organisms. *Marine Environmental Research*, 93, 106–117.  
920 <https://doi.org/10.1016/j.marenvres.2013.07.006>
- 921 Robledo Ardila, P. A., Álvarez-Alonso, R., Árcega-Cabrera, F., Durán Valsero, J. J., Morales García, R., Lamas-  
922 Cosío, E., Ocegüera-Vargas, I., & DelValls, A. (2024). Assessment and Review of Heavy Metals Pollution in  
923 Sediments of the Mediterranean Sea. *Applied Sciences*, 14(4). <https://doi.org/10.3390/app14041435>
- 924 Rodríguez-Ortega, M. J., Grøsvik, B. E., Rodríguez-Ariza, A., Goksøyr, A., & López-Barea, J. (2003). Changes in  
925 protein expression profiles in bivalve molluscs (*Chamaelea gallina*) exposed to four model environmental  
926 pollutants. *Proteomics*, 3(8), 1535–1543. <https://doi.org/10.1002/pmic.200300491>
- 927 Sacks, F. M. (2006). The apolipoprotein story. *Atherosclerosis Supplements*, 7(4), 23–27.  
928 <https://doi.org/10.1016/j.atherosclerosissup.2006.05.004>
- 929 Sakuragui, M. M., Paulino, M. G., Pereira, C. D. S., Carvalho, C. S., Sadauskas-Henrique, H., & Fernandes, M. N.  
930 (2013). Integrated use of antioxidant enzymes and oxidative damage in two fish species to assess  
931 pollution in man-made hydroelectric reservoirs. *Environmental Pollution*, 178, 41–51.  
932 <https://doi.org/10.1016/j.envpol.2013.02.032>
- 933 Sanchez, B. C., Ralston-Hooper, K., & Sepúlveda, M. S. (2011). Review of recent proteomic applications in  
934 aquatic toxicology. *Environmental Toxicology and Chemistry*, 30(2), 274–282.  
935 <https://doi.org/10.1002/etc.402>
- 936 Santos, C. R., & Schulze, A. (2012). Lipid metabolism in cancer. *FEBS Journal*, 279(15), 2610–2623.  
937 <https://doi.org/10.1111/j.1742-4658.2012.08644.x>
- 938 Saraux, C., Van Beveren, E., Brosset, P., Queiros, Q., Bourdeix, J.-H., Dutto, G., Gasset, E., Jac, C., Bonhommeau,  
939 S., & Fromentin, J.-M. (2019). Small pelagic fish dynamics: A review of mechanisms in the Gulf of Lions.  
940 *Deep Sea Research Part II: Topical Studies in Oceanography*, 159, 52–61.  
941 <https://doi.org/10.1016/j.dsr2.2018.02.010>
- 942 Sardenne, F., Bodin, N., Metral, L., Crottier, A., Le Grand, F., Bideau, A., Brisset, B., Bourjea, J., Saraux, C.,  
943 Bonhommeau, S., Kerzérho, V., Bernard, S., & Rouyer, T. (2019). Effects of extraction method and  
944 storage of dry tissue on marine lipids and fatty acids. *Analytica Chimica Acta*, 1051(November), 82–93.  
945 <https://doi.org/10.1016/j.aca.2018.11.012>
- 946 Sharma, S., Sharma, V., & Chatterjee, S. (2021). Microplastics in the Mediterranean Sea : Sources , Pollution  
947 Intensity , Sea Health , and Regulatory Policies. *Frontiers in Marine Science*, 8(May), 1–15.  
948 <https://doi.org/10.3389/fmars.2021.634934>
- 949 Si, L. F., Wang, C. C., Guo, S. N., Zheng, J. L., & Xia, H. (2019). The lagged effects of environmentally relevant  
950 zinc on non-specific immunity in zebrafish. *Chemosphere*, 214, 85–93.  
951 <https://doi.org/10.1016/j.chemosphere.2018.09.050>
- 952 Souid, G., Souayed, N., Yaktiti, F., & Maaroufi, K. (2015). Lead accumulation pattern and molecular biomarkers  
953 of oxidative stress in seabream ( *Sparus aurata* ) under short-term metal treatment. *Drug and Chemical*  
954 *Toxicology*, 38(1), 98–105. <https://doi.org/10.3109/01480545.2014.917091>
- 955 Strady, E., Harmelin-Vivien, M., Chiffolleau, J. F., Veron, A., Tronczynski, J., & Radakovitch, O. (2015). 210Po and  
956 210Pb trophic transfer within the phytoplankton-zooplankton-anchovy/sardine food web: A case study  
957 from the Gulf of Lion (NW Mediterranean Sea). *Journal of Environmental Radioactivity*, 143, 141–151.  
958 <https://doi.org/10.1016/j.jenvrad.2015.02.019>
- 959 Tang, W. L., Evans, D., Kraemer, L., & Zhong, H. (2017). Body size-dependent Cd accumulation in the zebra  
960 mussel *Dreissena polymorpha* from different routes. *Chemosphere*, 168, 825–831.

- 961 <https://doi.org/10.1016/j.chemosphere.2016.10.128>
- 962 Tchounwou, P. B., Yedjou, C. G., Patlolla, A. K., & Sutton, D. J. (2012). Heavy Metal Toxicity and the  
963 Environment. In A. Luch (Ed.), *Molecular, Clinical and Environmental Toxicology: Volume 3:*  
964 *Environmental Toxicology* (pp. 133–164). Springer Basel. [https://doi.org/10.1007/978-3-7643-8340-4\\_6](https://doi.org/10.1007/978-3-7643-8340-4_6)
- 965 Teulier, L., Thorat, E., Queiros, Q., McKenzie, D. J., Roussel, D., Dutto, G., Gasset, E., Bourjea, J., & Saraux, C.  
966 (2019). Muscle bioenergetics of two emblematic Mediterranean fish species: *Sardina pilchardus* and  
967 *Sparus aurata*. *Comparative Biochemistry and Physiology -Part A : Molecular and Integrative Physiology*,  
968 235, 174–179. <https://doi.org/10.1016/j.cbpa.2019.06.008>
- 969 Tocher, D. R. (2003). Metabolism and functions of lipids and fatty acids in teleost fish. In *Reviews in Fisheries*  
970 *Science* (Vol. 11, Issue 2, pp. 107–184). Taylor & Francis Group . <https://doi.org/10.1080/713610925>
- 971 Tournois, J., Darnaude, A. M., Ferraton, F., Aliaume, C., Mercier, L., & McKenzie, D. J. (2017). Lagoon nurseries  
972 make a major contribution to adult populations of a highly prized coastal fish. *Limnology and*  
973 *Oceanography*, 62(3), 1219–1233. <https://doi.org/10.1002/lno.10496>
- 974 Tronczynski, J., Carlotti, F., Bodin, N., & Radakovitch, O. (2013). Contaminants bioaccumulation and  
975 biomagnification in a short trophic system: phytoplankton, zooplankton, anchovy, sardine (COSTAS).  
976 *Ciesm*.
- 977 Van Beveren, E., Fromentin, J.-M., Rouyer, T., Bonhommeau, S., Brosset, P., & Saraux, C. (2016). The fisheries  
978 history of small pelagics in the Northern Mediterranean. *ICES Journal of Marine Science*, 73(6), 1475–  
979 1484. <https://doi.org/10.1093/ICESJMS/FSW023>
- 980 Van Beveren, E., Fromentin, J. M., Bonhommeau, S., Nieblas, A. E., Metral, L., Brisset, B., Jusup, M., Bauer, R.  
981 K., Brosset, P., & Saraux, C. (2017). Predator–prey interactions in the face of management regulations:  
982 Changes in Mediterranean small pelagic species are not due to increased tuna predation. *Canadian*  
983 *Journal of Fisheries and Aquatic Sciences*, 74(9), 1422–1430. <https://doi.org/10.1139/cjfas-2016-0152>
- 984 Van Beveren, E., Keck, N., Fromentin, J. M., Laurence, S., Boulet, H., Labrut, S., Baud, M., Bigarré, L., Brosset, P.,  
985 & Saraux, C. (2016). Can pathogens alter the population dynamics of sardine in the NW Mediterranean?  
986 *Marine Biology*, 163(12), 240. <https://doi.org/10.1007/s00227-016-3015-7>
- 987 Van Meer, G., Voelker, D. R., & Feigenson, G. W. (2008). Membrane lipids: Where they are and how they  
988 behave. *Nature Reviews Molecular Cell Biology*, 9(2), 112–124. <https://doi.org/10.1038/nrm2330>
- 989 Wang, L., & Gallagher, E. P. (2013). Role of Nrf2 antioxidant defense in mitigating cadmium-induced oxidative  
990 stress in the olfactory system of zebrafish. *Toxicology and Applied Pharmacology*, 266(2), 177–186.  
991 <https://doi.org/10.1016/j.taap.2012.11.010>
- 992 Wang, M., Wang, Y., Zhang, L., Wang, J., Hong, H., & Wang, D. (2013). Quantitative proteomic analysis reveals  
993 the mode-of-action for chronic mercury hepatotoxicity to marine medaka (*Oryzias melastigma*). *Aquatic*  
994 *Toxicology*, 130–131, 123–131. <https://doi.org/10.1016/j.aquatox.2013.01.012>
- 995 Wijesooriya, K., Jadaan, S. A., Perera, K. L., Kaur, T., & Ziemann, M. (2022). Urgent need for consistent  
996 standards in functional enrichment analysis. *PLOS Computational Biology*, 18(3), 1–14.  
997 <https://doi.org/10.1371/journal.pcbi.1009935>
- 998 Williams, C. R., & Yoshida-Honmachi, E. P. (2013). Effects of cadmium on olfactory mediated behaviors and  
999 molecular biomarkers in coho salmon (*Oncorhynchus kisutch*). *Aquatic Toxicology*, 140–141, 295–302.  
1000 <https://doi.org/10.1016/j.aquatox.2013.06.010>
- 1001 Wood, C. ., Farrell, A. ., & Brauner, C. . (2011). Copper of the Fish Physiology. In *Fish physiology* (pp. 55–133).

- 1002 Xu, L., Lu, Z., Ji, C., Cong, M., Li, F., Shan, X., & Wu, H. (2019). Toxicological effects of As (V) in juvenile rockfish  
1003 *Sebastes schlegelii* by a combined metabolomic and proteomic approach. *Environmental Pollution*, 255,  
1004 113333. <https://doi.org/10.1016/j.envpol.2019.113333>
- 1005 Yadetie, F., Karlsen, O. A., Lanzén, A., Berg, K., Olsvik, P., Hogstrand, C., & Goksøyr, A. (2013). Global  
1006 transcriptome analysis of Atlantic cod (*Gadus morhua*) liver after in vivo methylmercury exposure  
1007 suggests effects on energy metabolism pathways. *Aquatic Toxicology*, 126, 314–325.  
1008 <https://doi.org/10.1016/j.aquatox.2012.09.013>
- 1009 Yin, S., Liu, L., & Gan, W. (2021). The Roles of Post-Translational Modifications on mTOR Signaling.  
1010 *International Journal of Molecular Sciences*, 22(4). <https://doi.org/10.3390/ijms22041784>
- 1011 Zhol, S., Ackman, R. G., & Morrison, C. (1995). Storage of lipids in the myosepta of Atlantic salmon (*Salmo*  
1012 *salar*). *Fish Physiology and Biochemistry*, 14(2), 171–178. <https://doi.org/10.1007/BF00002460>
- 1013